

A Provable Splitting Approach for Symmetric Nonnegative Matrix Factorization

Xiao Li, Zhihui Zhu, Qiuwei Li, and Kai Liu

Abstract—The symmetric Nonnegative Matrix Factorization (NMF), a special but important class of the general NMF, has found numerous applications in data analysis such as various clustering tasks. Unfortunately, designing fast algorithms for the symmetric NMF is not as easy as for its nonsymmetric counterpart, since the latter admits the splitting property that allows state-of-the-art alternating-type algorithms. To overcome this issue, we first split the decision variable and transform the symmetric NMF to a penalized nonsymmetric one, paving the way for designing efficient alternating-type algorithms. We then show that solving the penalized nonsymmetric reformulation returns a solution to the original symmetric NMF. Moreover, we design a family of alternating-type algorithms and show that they all admit strong convergence guarantee: the generated sequence of iterates is convergent and converges at least sublinearly to a critical point of the original symmetric NMF. Finally, we conduct experiments on both synthetic data and real image clustering to support our theoretical results and demonstrate the performance of the alternating-type algorithms.

Index Terms—Symmetric nonnegative matrix factorization, convergence, image clustering, alternating minimization.



1 INTRODUCTION

The general nonsymmetric Nonnegative Matrix Factorization (NMF) is referred to the following problem: given a matrix $\mathbf{Y} \in \mathbb{R}^{n \times m}$ and a factorization rank r , solve

$$\min_{\mathbf{U} \in \mathbb{R}^{n \times r}, \mathbf{V} \in \mathbb{R}^{m \times r}} \frac{1}{2} \|\mathbf{Y} - \mathbf{UV}^T\|_F^2 \quad (1)$$

subject to $\mathbf{U} \geq \mathbf{0}, \mathbf{V} \geq \mathbf{0}$,

where $\mathbf{U} \geq \mathbf{0}$ means each element in \mathbf{U} is nonnegative. NMF has been successfully used in the applications of face feature extraction [2], [3], document clustering [4]–[6], image clustering [7], [8], music analysis [9], source separation [10] and many others [11]. Because of the ubiquitous applications of NMF, many efficient algorithms have been proposed for solving problem (1). Well-known algorithms include multiplicative update algorithm [12], Projected Gradient Descent (PGD) [13], Alternating Nonnegative Least Squares (ANLS) [14], and Hierarchical Alternating Least Squares

(HALS) [15]. In particular, ANLS (which uses the block principal pivoting algorithm to very efficiently solve the nonnegative least squares) and HALS achieve the state-of-the-art performance.

One special but important class of NMF, called symmetric NMF, requires the two factors \mathbf{U} and \mathbf{V} to be identical, i.e., it factorizes a symmetric matrix $\mathbf{X} \in \mathbb{R}^{n \times n}$ by solving

$$\min_{\mathbf{U} \in \mathbb{R}^{n \times r}} \frac{1}{2} \|\mathbf{X} - \mathbf{UU}^T\|_F^2, \quad \text{subject to } \mathbf{U} \geq \mathbf{0}. \quad (2)$$

By contrast, (1) is referred to as the general nonsymmetric NMF. Symmetric NMF has its own applications in data analysis, machine learning and signal processing [16]–[20]. In particular the symmetric NMF is equivalent to the classical K -means kernel clustering in [16] and it is inherently suitable for clustering nonlinearly separable data from a symmetric similarity matrix [18].

At first glance, since (2) has only one variable, one may think it is easier to be solved than (1) or at least it can be solved by directly utilizing efficient algorithms developed for (1). However, the state-of-the-art alternating-type algorithms (such as ANLS and HALS) for solving the general nonsymmetric NMF utilize the splitting property of the decision variables in (1) and thus can not be used for tackling (2). On the other hand, first order method like PGD when used to solve (2) suffers from slow convergence.

1.1 Main Contributions

In this paper, we compute the symmetric NMF by considering a variable splitting method, which reformulates our problem to a penalized nonsymmetric NMF. This new nonsymmetric reformulation enables us to design efficient alternating-type algorithms for solving the original symmetric NMF. The main contributions of this paper are summarized as follows.

- Motivated by the splitting property exploited in ANLS and HALS algorithms, we split the quadratic form on

X. Li is with School of Data Science, The Chinese University of Hong Kong, Shenzhen and is with Shenzhen Institute of Artificial Intelligence and Robotics for Society (AIRS) (e-mail: lixiao@cuhk.edu.cn).

Z. Zhu is with the Department of Electrical and Computer Engineering at the University of Denver. (corresponding author. e-mail: zhihui.zhu@du.edu).

Q. Li is with the Decision Intelligence Lab, Damo Academy, Alibaba Group US. (e-mail: liqiuweiss@gmail.com).

K. Liu is with Computer Science Division, Clemson University. (e-mail: liukaizhijia@gmail.com).

Part of this work appears in a conference proceeding [1]. This work significantly extends the preliminary conference version. We have three new contributions compared to the conference version: 1) We propose the new accelerated SymHALS (A-SymHALS) algorithm. 2) We provide a unified convergence analysis that guarantees sequence convergence for all of our algorithms. The standard convergence analysis technique used in [1] cannot be directly applied due to the specific updating scheme of A-SymHALS. We provide a new analysis framework that is different from the existing standard one and is of independent interest; see the last paragraph of Section 1.1 for details. 3) We propose a new adaptive strategy for updating the penalty parameter λ . This adaptive strategy could be crucial for the practical use of our algorithms for solving symmetric NMF as it avoids hyper-parameter tuning. In addition to the above three important new contributions, we also conduct more experiments in this work.

U in the symmetric NMF into two different factors and transform symmetric NMF to a penalized nonsymmetric NMF, i.e.,

$$\min_{U, V} g(U, V) = \frac{1}{2} \|X - UV^T\|_F^2 + \frac{\lambda}{2} \|U - V\|_F^2 \quad (3)$$

subject to $U \geq 0, V \geq 0$,

where the penalty term $\|U - V\|_F^2$ is introduced to force the two factors identical and $\lambda > 0$ is the penalty parameter. Our first main contribution is to guarantee that with a sufficiently large but *finite* λ , any *critical point* (U^*, V^*) of (3) that has bounded energy (where the upper bound depends on λ) satisfies that (i) $U^* = V^*$ and (ii) U^* is a critical point of the symmetric NMF (2). The result is surprising in the sense that classical result of the methods of Lagrangian multipliers suggests that the two factors will be identical only when λ tends to *infinity* since the quadratic penalty is not an exact penalty function [21, Theorem 17.1].

- We further show that any algorithm possessing descent and convergence properties for solving (3) is guaranteed to yield a critical point of (2), provided that the penalty parameter λ is properly chosen. In summary, this observation suggests that the symmetric NMF can be provably solved by instead addressing the nonsymmetric NMF (3) which enjoys the splitting property within the factors U and V .
- Motivated by ANLS, HALS, and accelerated HALS [22], we then design a family of alternating-type algorithms—namely the Symmetric Alternating Nonnegative Least Squares (SymANLS; see Algorithm 1), the Symmetric Hierarchical Alternating Least Squares (SymHALS; see Algorithm 2), and the Accelerated Symmetric Hierarchical Alternating Least Squares (A-SymHALS; see Algorithm 3)—to solve the penalized nonsymmetric NMF (3). Our third contribution is to provide a unified rigorous convergence analysis for these three algorithms. By exploiting the specific structure of (3), we show that our proposed algorithms are guaranteed to sequentially decrease the objective function in (3) even without any proximal terms or any additional boundedness constraints on U and V . Consequently, we establish the point-wise *sequence convergence* to a critical point (U^*, V^*) of (3), where the convergence rate is at least *sublinear*. Finally, it is worth mentioning that the disciplined Kurdyka-Lojasiewicz convergence analysis framework [23], [24] cannot be directly applied to A-SymHALS due to its acceleration scheme, i.e., it updates one variable multiple times before moving to the other variable. We generalize this convergence analysis framework to accommodate this accelerate scheme, which is of independent interest.

1.2 Related Work

Due to slow convergence of PGD for solving the symmetric NMF, several algorithms have been proposed, either in a direct way or similar to (3) by splitting the two factors. The authors in [25] proposed an alternating algorithm that cyclically optimizes over each element in U by solving a nonnegative constrained nonconvex univariate fourth order polynomial minimization. A quasi newton second order

method was used in [18] to directly solve the symmetric NMF optimization problem (2). However, both the element-wise updating approach and the second order method are computationally expensive for large scale applications. In [17], the authors designed an accelerated multiplicative update algorithm, while in [26] the authors proposed an Singular Value Decomposition (SVD)-based algorithm that iteratively approximates the symmetric NMF. Nevertheless, the experiments in Section 4 indicate that they tend to get stuck at local minima with large fitting errors for noisy data.

The idea of solving symmetric NMF by targeting the penalized nonsymmetric NMF (3) also appears *heuristically* in [18]. The ANLS algorithm is used in [18] for solving (3), but without any formal analysis for the convergence and the question that whether solving (3) returns a solution of (2). The work [20], [27], [28] considered an augmented Lagrangian formulation of (2) that also enjoys the splitting property as in (3) by splitting the quadratic form UU^T into UV^T and introducing an equality constraint (i.e., $U = V$), and utilized the Alternating Direction Method of Multipliers (ADMM) or its variants to tackle the corresponding problem. Unlike the alternating-type algorithms for (3) that will be proved to have sequence convergence in Section 3, however, the ADMM is only guaranteed to have a subsequence convergence, even with an additional proximal term¹ and assumption on the boundedness of the iterates [20] or a constraint on the boundedness of columns of U [28], rendering the problem hard to solve.

Our work is also closely related to recent advances in convergence analysis for alternating minimization algorithms. The work [23] established sequence convergence for general alternating minimization algorithms with an additional proximal term and a boundedness assumption on the iterates. When specified to NMF, as pointed out in [29], with the aid of an additional proximal term as well as an additional constraint bounding the factors, the sequence convergence of ANLS and HALS can be established from [23], [30]. Although the convergence of these algorithms are observed without the proximal term and bounded constraint (which are indeed not used in practice), these are in general necessary to formally show the convergence of the algorithms. By contrast, without any additional constraint, the presence of the penalty term $\|U - V\|_F^2$ allows us to show that (i) our proposed algorithms admit the so-called sufficient decrease property, and consequently, (ii) the iterates generated by our algorithms are indeed bounded along the iterations. These observations then guarantee the sequence convergence of the practical algorithms without those additional constraint or proximal terms.

2 TRANSFORMING SYMMETRIC NMF TO PENALIZED NONSYMMETRIC NMF

2.1 Notations

We begin by introducing some notations. For the purpose of technical analysis, we may rewrite (3) as an unconstrained

¹ In k -th iteration, a proximal term (e.g., $\|U - U_{k-1}\|_F^2$) is added to the objective function when updating U in [28] and when updating both U and V in [20].

optimization problem using indicator function,

$$\min_{\mathbf{U}, \mathbf{V}} f(\mathbf{U}, \mathbf{V}) = g(\mathbf{U}, \mathbf{V}) + \sigma_+(\mathbf{U}) + \sigma_+(\mathbf{V}),$$

with σ_+ being the indicator function of nonnegative constraint defined as $\sigma_+(\mathbf{V}) = \begin{cases} 0, & \mathbf{V} \geq 0, \\ +\infty, & \text{otherwise,} \end{cases}$. Upper boldface (such as \mathbf{U}) and lower boldface (such as \mathbf{u}) respectively denote matrices and vectors in real Euclidean space. $\mathbf{A} \odot \mathbf{B}$ represents the Hadamard product of two matrices. $\langle \mathbf{A}, \mathbf{B} \rangle = \text{trace}(\mathbf{A}^\top \mathbf{B})$ represents the inner product of two matrices. Throughout this paper, k represents the iteration number only.

2.2 Penalized Nonsymmetric NMF is Equivalent to Symmetric NMF

Compared with (2), at first glance, (3) is slightly more complicated as it has one more variable. However, because of this new variable, $f(\mathbf{U}, \mathbf{V})$ is now strongly convex with respect to either \mathbf{U} or \mathbf{V} , though it is still nonconvex in terms of the joint variable (\mathbf{U}, \mathbf{V}) . Moreover, the two decision variables \mathbf{U} and \mathbf{V} in (3) are well separated, as the case in the general nonsymmetric NMF. This observation suggests an interesting and useful fact that (3) can be solved by tailored alternating-type algorithms. On the other hand, a theoretical question raised in the penalized nonsymmetric form (3) is whether we are guaranteed $\mathbf{U} = \mathbf{V}$ and hence solving (3) is equivalent to solving (2). In this section, we provide an assuring answer to this question that solving (3) (to a critical point) indeed gives a critical point solution of (2). Note that problem (2) is nonconvex, and thus many local search algorithms can only be guaranteed to converge to its critical point rather than global minimizer.

Before stating out the formal result, we first consider a simple case, as an intuitive example, where $f(u, v) = (1 - uv)^2/2 + \lambda(u - v)^2/2$. Its derivative is $\partial_u f(u, v) = (uv - 1)v + \lambda(u - v)$, $\partial_v f(u, v) = (uv - 1)u - \lambda(u - v)$. Thus, any critical point of f satisfies $(uv - 1)v + \lambda(u - v) = 0$ and $(uv - 1)u - \lambda(u - v) = 0$, further indicating that $(u - v)(2\lambda + 1 - uv) = 0$. Therefore, for any critical point (u, v) such that $|uv| < 2\lambda + 1$, it must satisfy $u = v$. Although (3) is more complicated as it also has nonnegative constraint, the following result establishes similar guarantee for (3).

Theorem 1. *Let $(\mathbf{U}^*, \mathbf{V}^*)$ be any critical point of (3) satisfying $\|\mathbf{U}^* \mathbf{V}^{*\top}\|_2 < 2\lambda + \sigma_n(\mathbf{X})$, where $\|\cdot\|_2$ denotes the spectral norm and $\sigma_i(\cdot)$ denotes the i -th largest eigenvalue. Then $\mathbf{U}^* = \mathbf{V}^*$ and \mathbf{U}^* is a critical point of (2).*

Proof of Theorem 1. We first present the following useful result for any symmetric $\mathbf{A} \in \mathbb{R}^{n \times n}$ and PSD matrix $\mathbf{B} \in \mathbb{R}^{n \times n}$ [31, Lemma 1],

$$\sigma_n(\mathbf{A}) \text{trace}(\mathbf{B}) \leq \text{trace}(\mathbf{A}\mathbf{B}) \leq \sigma_1(\mathbf{A}) \text{trace}(\mathbf{B}). \quad (4)$$

We now prove Theorem 1. The subdifferential of f is given as follows

$$\begin{aligned} \partial_{\mathbf{U}} f(\mathbf{U}, \mathbf{V}) &= (\mathbf{U}\mathbf{V}^\top - \mathbf{X})\mathbf{V} + \lambda(\mathbf{U} - \mathbf{V}) + \partial\delta_+(\mathbf{U}), \\ \partial_{\mathbf{V}} f(\mathbf{U}, \mathbf{V}) &= (\mathbf{U}\mathbf{V}^\top - \mathbf{X})^\top \mathbf{U} - \lambda(\mathbf{U} - \mathbf{V}) + \partial\delta_+(\mathbf{V}), \end{aligned} \quad (5)$$

where $\partial\delta_+(\mathbf{U}) = \{\mathbf{G} \in \mathbb{R}^{n \times r} : \mathbf{G} \odot \mathbf{U} = \mathbf{0}, \mathbf{G} \leq \mathbf{0}\}$ when $\mathbf{U} \geq \mathbf{0}$ and otherwise $\partial\delta_+(\mathbf{U}) = \emptyset$. Since $(\mathbf{U}^*, \mathbf{V}^*)$ is a critical point of (3), it satisfies

$$(\mathbf{U}^* \mathbf{V}^{*\top} - \mathbf{X})\mathbf{V}^* + \lambda(\mathbf{U}^* - \mathbf{V}^*) + \mathbf{G} = \mathbf{0}, \quad (6)$$

$$(\mathbf{U}^* \mathbf{V}^{*\top} - \mathbf{X})^\top \mathbf{U}^* - \lambda(\mathbf{U}^* - \mathbf{V}^*) + \mathbf{H} = \mathbf{0}, \quad (7)$$

where $\mathbf{G} \in \partial\delta_+(\mathbf{U}^*)$ and $\mathbf{H} \in \partial\delta_+(\mathbf{V}^*)$. Subtracting (7) from (6), we have

$$\begin{aligned} (2\lambda\mathbf{I} + \mathbf{X})(\mathbf{U}^* - \mathbf{V}^*) \\ = \mathbf{V}^* \mathbf{U}^{*\top} \mathbf{U}^* - \mathbf{U}^* \mathbf{V}^{*\top} \mathbf{V}^* - \mathbf{G} + \mathbf{H}. \end{aligned} \quad (8)$$

where we utilized the fact that \mathbf{X} is symmetric, i.e., $\mathbf{X} = \mathbf{X}^\top$. Taking the inner product of $\mathbf{U}^* - \mathbf{V}^*$ with both sides of the above equation gives

$$\begin{aligned} \langle (\lambda\mathbf{I} + \mathbf{X}), (\mathbf{U}^* - \mathbf{V}^*)(\mathbf{U}^* - \mathbf{V}^*)^\top \rangle \\ = \langle \mathbf{V}^* \mathbf{U}^{*\top} \mathbf{U}^* - \mathbf{U}^* \mathbf{V}^{*\top} \mathbf{V}^* - \mathbf{G} + \mathbf{H}, \mathbf{U}^* - \mathbf{V}^* \rangle. \end{aligned} \quad (9)$$

In what follows, by choosing sufficiently large λ , we show that $(\mathbf{U}^*, \mathbf{V}^*)$ satisfying (9) must satisfy $\mathbf{U}^* = \mathbf{V}^*$. To that end, we first provide the lower bound and the upper bound for the left-hand side and right-hand side of (9), respectively. Specifically,

$$\begin{aligned} \langle ((2\lambda\mathbf{I} + \mathbf{X}), (\mathbf{U}^* - \mathbf{V}^*)(\mathbf{U}^* - \mathbf{V}^*)^\top) \rangle \\ \geq \sigma_n((2\lambda\mathbf{I} + \mathbf{X})) \|\mathbf{U}^* - \mathbf{V}^*\|_F^2 \\ = ((2\lambda + \sigma_n(\mathbf{X})) \|\mathbf{U}^* - \mathbf{V}^*\|_F^2, \end{aligned} \quad (10)$$

where the inequality follows from (4). On the other hand,

$$\begin{aligned} \langle \mathbf{V}^* \mathbf{U}^{*\top} \mathbf{U}^* - \mathbf{U}^* \mathbf{V}^{*\top} \mathbf{V}^* - \mathbf{G} + \mathbf{H}, \mathbf{U}^* - \mathbf{V}^* \rangle \\ \leq \langle \mathbf{V}^* \mathbf{U}^{*\top} \mathbf{U}^* - \mathbf{U}^* \mathbf{V}^{*\top} \mathbf{V}^*, \mathbf{U}^* - \mathbf{V}^* \rangle \\ = \left\langle \frac{\mathbf{V}^* \mathbf{U}^{*\top} + \mathbf{U}^* \mathbf{V}^{*\top}}{2}, (\mathbf{U}^* - \mathbf{V}^*)(\mathbf{U}^* - \mathbf{V}^*)^\top \right\rangle \\ - \frac{1}{2} \left\| \mathbf{U}^* \mathbf{V}^{*\top} - \mathbf{V}^* \mathbf{U}^{*\top} \right\|_F^2 \\ \leq \left\langle \frac{\mathbf{V}^* \mathbf{U}^{*\top} + \mathbf{U}^* \mathbf{V}^{*\top}}{2}, (\mathbf{U}^* - \mathbf{V}^*)(\mathbf{U}^* - \mathbf{V}^*)^\top \right\rangle \\ \leq \sigma_1 \left(\frac{\mathbf{V}^* \mathbf{U}^{*\top} + \mathbf{U}^* \mathbf{V}^{*\top}}{2} \right) \|\mathbf{U}^* - \mathbf{V}^*\|_F^2, \end{aligned} \quad (11)$$

where the last inequality utilizes (4) and the first inequality follows because $\mathbf{V}^*, \mathbf{U}^* \geq \mathbf{0}$ indicating that

$$-\langle \mathbf{G}, \mathbf{U}^* - \mathbf{V}^* \rangle \leq 0, \quad \langle \mathbf{H}, \mathbf{U}^* - \mathbf{V}^* \rangle \leq 0.$$

Now plugging (10) and (11) back into (9) and using the fact that $\sigma_1 \left(\frac{\mathbf{V}^* \mathbf{U}^{*\top} + \mathbf{U}^* \mathbf{V}^{*\top}}{2} \right) \leq \|\mathbf{U}^* \mathbf{V}^{*\top}\|_2$, we have

$$\begin{aligned} ((2\lambda + \sigma_n(\mathbf{X})) \|\mathbf{U}^* - \mathbf{V}^*\|_F^2 \\ \leq \sigma_1 \left(\frac{\mathbf{V}^* \mathbf{U}^{*\top} + \mathbf{U}^* \mathbf{V}^{*\top}}{2} \right) \|\mathbf{U}^* - \mathbf{V}^*\|_F^2 \\ \leq \|\mathbf{U}^* \mathbf{V}^{*\top}\|_2 \|\mathbf{U}^* - \mathbf{V}^*\|_F^2, \end{aligned}$$

which implies that if we choose $2\lambda > \|\mathbf{U}^* \mathbf{V}^{*\top}\|_2 - \sigma_n(\mathbf{X})$, then $\mathbf{U}^* = \mathbf{V}^*$ must hold. Plugging it into (5) gives

$$\mathbf{0} \in (\mathbf{U}^* (\mathbf{U}^*)^\top - \mathbf{X}) \mathbf{U}^* + \partial\delta_+(\mathbf{U}^*),$$

which implies \mathbf{U}^* is a critical point of (2). \square

Several remarks on Theorem 1 are made as follows. First, the strategy of solving the symmetric NMF by targeting on a nonsymmetric one can be naturally extended to multiple variables, such as symmetric tensor factorization. Investigation along this line is of interest and is the subject of future work. Also, note that for any $\lambda > 0$, Theorem 1 ensures a certain region (whose size depends on λ) in which each critical point of (3) has identical factors and also returns a solution for the original symmetric NMF (2). This further suggests the opportunity of choosing an appropriate λ such that the corresponding region (i.e., all (\mathbf{U}, \mathbf{V}) such that $\|\mathbf{U}\mathbf{V}^T\| < 2\lambda + \sigma_n(\mathbf{X})$) contains all the possible points that the algorithms will converge to. The rest is to argue that for any local search algorithms when used to solve (3), if it decreases the objective function, then the iterates are bounded.

Lemma 1. *For any local search algorithm solving (3) with initialization $\mathbf{V}_0 = \mathbf{U}_0, \mathbf{U}_0 \geq 0$, suppose it sequentially decreases the objective value. Then, for any $k \geq 0$, the iterate $(\mathbf{U}_k, \mathbf{V}_k)$ generated by this algorithm satisfies*

$$\begin{aligned} \|\mathbf{U}_k\|_F^2 + \|\mathbf{V}_k\|_F^2 &\leq \left(\frac{1}{\lambda} + 2\sqrt{r}\right) \|\mathbf{X} - \mathbf{U}_0\mathbf{U}_0^T\|_F^2 \\ &\quad + 2\sqrt{r}\|\mathbf{X}\|_F := B_0, \\ \|\mathbf{U}_k\mathbf{V}_k^T\|_2 &\leq \|\mathbf{X} - \mathbf{U}_0\mathbf{U}_0^T\|_F + \|\mathbf{X}\|_2. \end{aligned} \quad (12)$$

Proof of Lemma 1. By the assumption that the algorithm decreases the objective function, we have

$$\frac{1}{2} \|\mathbf{X} - \mathbf{U}_k\mathbf{V}_k^T\|_F^2 + \frac{\lambda}{2} \|\mathbf{U}_k - \mathbf{V}_k\|_F^2 \leq \frac{1}{2} \|\mathbf{X} - \mathbf{U}_0\mathbf{U}_0^T\|_F^2$$

which further implies that

$$\|\mathbf{X} - \mathbf{U}_k\mathbf{V}_k^T\|_F \leq \|\mathbf{X} - \mathbf{U}_0\mathbf{U}_0^T\|_F, \quad (13)$$

and

$$\begin{aligned} &\frac{\lambda}{2} \left(\|\mathbf{U}_k\|_F^2 + \|\mathbf{V}_k\|_F^2 - 2|\langle \mathbf{U}_k\mathbf{V}_k^T, \mathbf{I}_r \rangle| \right) \\ &= \frac{\lambda}{2} \|\mathbf{U}_k - \mathbf{V}_k\|_F^2 \leq \frac{1}{2} \|\mathbf{X} - \mathbf{U}_0\mathbf{U}_0^T\|_F^2. \end{aligned} \quad (14)$$

It follows from (13) that

$$\begin{aligned} \|\mathbf{U}_k\mathbf{V}_k^T\|_2 - \|\mathbf{X}\|_2 &\leq \|\mathbf{U}_k\mathbf{V}_k^T - \mathbf{X}\|_2 \leq \|\mathbf{U}_k\mathbf{V}_k^T - \mathbf{X}\|_F \\ &\leq \|\mathbf{X} - \mathbf{U}_0\mathbf{U}_0^T\|_F. \end{aligned}$$

Also, the inequality in (14) leads to

$$\begin{aligned} \|\mathbf{U}_k\|_F^2 + \|\mathbf{V}_k\|_F^2 &\leq \frac{1}{\lambda} \|\mathbf{X} - \mathbf{U}_0\mathbf{U}_0^T\|_F^2 + 2\|\mathbf{U}_k\mathbf{V}_k^T\|_F \|\mathbf{I}_r\|_F \\ &= \frac{1}{\lambda} \|\mathbf{X} - \mathbf{U}_0\mathbf{U}_0^T\|_F^2 + 2\sqrt{r}\|\mathbf{U}_k\mathbf{V}_k^T\|_F \\ &\leq \left(\frac{1}{\lambda} + 2\sqrt{r}\right) \|\mathbf{X} - \mathbf{U}_0\mathbf{U}_0^T\|_F^2 + 2\sqrt{r}\|\mathbf{X}\|_F \\ &=: B_0 \end{aligned}$$

□

There are two interesting facts regarding the iterates that can be interpreted from (12). The first equation of (12) implies that both \mathbf{U}_k and \mathbf{V}_k are bounded and the upper bound decays when the λ increases. Specifically, as long as λ is not too close to zero, then the right-hand side in (12) gives

a meaningful bound which will be used for the convergence analysis of local search algorithms in next section. In terms of $\mathbf{U}_k\mathbf{V}_k^T$, the second equation of (12) indicates that it is indeed upper bounded by a quantity that is independent of λ . This suggests a key result that if the iterative algorithm is convergent and the iterates $(\mathbf{U}_k, \mathbf{V}_k)$ converge to a critical point $(\mathbf{U}^*, \mathbf{V}^*)$, then $\mathbf{U}^*\mathbf{V}^{*T}$ is also bounded, irrespectively the value of λ . This together with Theorem 1 ensures that many local search algorithms can be utilized to find a critical point of (2) by targeting (3) with a properly chosen large λ .

Theorem 2. *In (3), set*

$$\lambda > \frac{1}{2} \left(\|\mathbf{X}\|_2 + \|\mathbf{X} - \mathbf{U}_0\mathbf{U}_0^T\|_F - \sigma_n(\mathbf{X}) \right). \quad (15)$$

For any local search algorithm solving (3) with initialization $\mathbf{V}_0 = \mathbf{U}_0$, if it sequentially decreases the objective function, is convergent, and converges to a critical point $(\mathbf{U}^, \mathbf{V}^*)$ of (3), then we have $\mathbf{U}^* = \mathbf{V}^*$ and \mathbf{U}^* is also a critical point of (2).*

Proof of Theorem 2. Since the assumptions of Lemma 1 are satisfied, it follows from (12) that

$$\begin{aligned} \|\mathbf{U}^*\mathbf{V}^{*T}\|_2 &\leq \|\mathbf{X} - \mathbf{U}_0\mathbf{U}_0^T\|_F + \|\mathbf{X}\|_2 \\ &< 2\lambda + \sigma_n(\mathbf{X}), \end{aligned}$$

where the second line utilizes (15). We complete the proof by invoking Theorem 1. □

Remark 1. Theorem 2 indicates that instead of directly solving the symmetric NMF (2), one can turn to solve (3) with a properly chosen penalty parameter λ . The latter has similar form to the general nonsymmetric NMF (1) obeying splitting property, which paves the way for designing efficient alternating-type algorithms.

3 FAST ALGORITHMS FOR SYMMETRIC NMF

In the last section, we have shown that the symmetric NMF (2) can be transformed to problem (3) which admits splitting property, enabling us to design efficient alternating-type algorithms to solve the original symmetric NMF. In this section, we exploit the splitting property and design fast algorithms for solving problem (3) by adopting ANLS, HALS, and accelerated HALS. Moreover, we provide strong convergence guarantees that the sequence of iterates generated by our algorithms is convergent and converges to a critical point of the original symmetric NMF (2). This is obtained by exploiting Theorem 2 and the property that the objective function f in (3) is strongly convex with respect to \mathbf{U} (or \mathbf{V}) when the other variable \mathbf{V} (or \mathbf{U}) is fixed.

3.1 ANLS-type Method for Symmetric NMF

ANLS is an alternating-type algorithm customized for nonsymmetric NMF (1) and its main idea is to keep one factor fixed and update another one via solving a nonnegative least squares. We use a similar idea for solving (3) and refer to the corresponding algorithm as SymANLS; see Algorithm 1. Specifically, at the k -th iteration, SymANLS first updates \mathbf{U}_k by

$$\mathbf{U}_k = \arg \min_{\mathbf{U} \in \mathbb{R}^{n \times r}, \mathbf{U} \geq 0} \|\mathbf{X} - \mathbf{U}\mathbf{V}_{k-1}^T\|_F^2 + \frac{\lambda}{2} \|\mathbf{U} - \mathbf{V}_{k-1}\|_F^2. \quad (16)$$

Algorithm 1 SymANLS**Initialization:** $k = 1$ and $U_0 = V_0$.

- 1: **while** stop criterion not meet **do**
- 2: $U_k = \arg \min_{U \geq 0} \frac{1}{2} \|X - UV_{k-1}^T\|_F^2 + \frac{\lambda}{2} \|U - V_{k-1}\|_F^2$;
- 3: $V_k = \arg \min_{V \geq 0} \frac{1}{2} \|X - U_k V^T\|_F^2 + \frac{\lambda}{2} \|U_k - V\|_F^2$;
- 4: $k = k + 1$.
- 5: **end while**

Output: factorization (U_k, V_k) .

V_k is then updated in a similar way. For solving the subproblem (16), we first note that there exists a unique minimizer (i.e., U_k) for (16) as it involves a strongly objective function as well as a convex constraint. Unlike least squares, however, in general there is no closed-form solution for (16) (unless $r = 1$) due to the nonnegative constraint. Fortunately, there exist many feasible methods to solve the nonnegative least squares, such as projected gradient descent, active set method and projected Newton's method. Among these methods, a block principal pivoting method is remarkably efficient for tackling the subproblem (16) (and also the one for updating V) [14].

Algorithm 2 SymHALS**Initialization:** $k = 1$ and $U_0 = V_0$.

- 1: precompute residual $\bar{X}_k = X - U_{k-1}V_{k-1}^T$.
- 2: **while** stop criterion not meet **do**
- 3: **for** $i = 1 : r$ **do**
- 4: $\bar{X}_k \leftarrow \bar{X}_k + \mathbf{u}_{i,k-1}(\mathbf{v}_{i,k-1})^T$
- 5: $\mathbf{u}_{i,k} = \max\left(\frac{(\bar{X}_k + \lambda \mathbf{I})\mathbf{v}_{i,k-1}}{\|\mathbf{v}_{i,k-1}\|_2 + \lambda}, 0\right)$;
- 6: Update residual $\bar{X}_k \leftarrow \bar{X}_k - \mathbf{u}_{i,k}(\mathbf{v}_{i,k-1})^T$.
- 7: **end for**
- 8: Update V_k using the same steps.
- 9: $\bar{X}_{k+1} = \bar{X}_k$, $k = k + 1$.
- 10: **end while**

Output: factorization (U_k, V_k) .**3.2 Accelerated HALS-type Method for Symmetric NMF**

Compared with ANLS, HALS may need more iterations to converge since in each step it only updates one column. One effective approach [22] to accelerate HALS is by updating one block variable (say U) several times before processing another block variable (say V), i.e., cyclically updating $\mathbf{u}_1, \dots, \mathbf{u}_r$ by (??) multiple times before updating V . We adopt this strategy and denote the corresponding algorithm by A-SymHALS, which is depicted in Algorithm 3.

Remark 2. SymHALS updates each column of U and V one time during each iteration, while A-SymHALS updates each column multiple times by refining previous solutions. Thus, on the one hand, A-SymHALS has higher computational complexity than SymHALS in each iteration, but less than SymANLS since the latter requires to solve relatively computationally expensive nonnegative least squares in each iteration. On the other hand, A-SymHALS is supposed to converge faster than SymHALS since the former decreases more function value in each iteration, while SymANLS can decrease the most function value among them in each

Algorithm 3 A-SymHALS**Initialization:** $k = 1$ and $U_0 = V_0$, and inner iteration number L .

- 1: **while** stop criterion not meet **do**
- 2: Inner initialization: $U_k^0 = U_k$
- 3: **for** $j = 1 : L$ **do**
- 4: Update U_k^j by performing steps 3-7 in Algorithm 2 with V_k and U_k^{j-1} .
- 5: **end for**
- 6: Set $U_{k+1} = U_k^L$.
- 7: Repeat the above process (steps 2-6) to update V_{k+1} .
- 8: $k = k + 1$.
- 9: **end while**

Output: factorization (U_k, V_k) .

iteration. Therefore, A-SymHALS can be viewed as an effective approach to balance the trade-off between convergence speed and computational complexity of each iteration within SymHALS and SymANLS. We will compare these three algorithms in Section 4. But before this, in the next Section we provide convergence analysis for the three algorithms and show that all of them will converge to a critical point of the original symmetric NMF problem (2).

3.3 Convergence Results

By exploiting the strong convexity of the objective function in (3) when restricted to block U (or V) and the guarantee of Theorem 2, we establish the convergence result of the three proposed alternating algorithms.

Theorem 3 (Convergence of the proposed algorithms to a critical point of the symmetric NMF (2)). *In (3), set*

$$\lambda > \frac{1}{2} \left(\|X\|_2 + \|X - U_0 U_0^T\|_F - \sigma_n(X) \right) =: \bar{\lambda}. \quad (17)$$

Suppose Algorithm 1, Algorithm 2, and Algorithm 3 are initialized with $V_0 = U_0$. Let $\{(U_k, V_k)\}_{k \geq 0}$ be the sequence of iterates generated by any of the three algorithms. Then,

$$\lim_{k \rightarrow \infty} (U_k, V_k) = (U^*, V^*),$$

where the limit point (U^, V^*) satisfies $U^* = V^*$ and U^* is a critical point of (2). Furthermore, the convergence rate is at least sublinear.*

The proof of Theorem 3 consists of showing the convergence requirement of algorithms in Theorem 2; i.e., the decent and convergence properties. We defer the detailed proof to Section 5.

Remark 3. First note that the algorithm can be proved to converge to (U^*, V^*) for any positive λ with the argument in Section 5, but we need λ to be relatively large as in (17) to ensure $U^* = V^*$. We emphasize that the specific structure within (3) enables Theorem 3 to get rid of both the assumption on the boundedness of the iterates $\{(U_k, V_k)\}_{k \geq 0}$ and the requirement of an additional proximal term, which are usually required for convergence analysis though are not necessary in practice [23], [32]. For example, the previous work [29] provides convergence guarantee for the standard ANLS when used to solve the general nonsymmetric NMF

(1) by adding an additional proximal term as well as an additional constraint to force the factors bounded. To establish the convergence for the standard HALS for solving (1) [15], [22], one needs the assumption that every column in $(\mathbf{U}_k, \mathbf{V}_k)$ is away from zero through all iterations. Though such an assumption can be satisfied by explicitly imposing additional constraints, it leads to a slightly different problem. By contrast, our convergence result when applied to SymHALS and A-SymHALS overcomes this issue because of the additional penalty term in (3).

Remark 4. The convergence of SymANLS and SymHALS can be established by following the Kurdyka-Lojasiewicz (KL) convergence analysis framework [23], [24] since the additional penalty term in (3) can be used for establishing the so-called sufficient decrease property of the two algorithms. However, the multiple update scheme of A-SymHALS makes its convergence analysis more complicated than the previous two algorithms. As a result, one cannot directly apply this framework for A-SymHALS. To overcome this technical difficulty, we generalize the KL analysis framework such that it becomes compatible with the multiple update scheme used in A-SymHALS, which is of independent interest; see Section 5 for detailed analysis.

3.4 An Adaptive Updating Formula for λ

Theorem 3 guarantees convergence of the three algorithms for any relatively large penalty parameter λ . Though λ is fixed in Algorithms 1-3 for simplicity, it can be updated through the entire process. In this subsection, we provide an adaptive strategy for updating the parameter λ along with the iterations of our algorithms. Towards that end, first note that $\|\mathbf{U}_k \pm \mathbf{V}_k\|_F^2 \geq 0$ always holds, which gives

$$\|\mathbf{U}_k\|_F^2 + \|\mathbf{V}_k\|_F^2 \geq 2|\langle \mathbf{U}_k, \mathbf{V}_k \rangle|.$$

This further implies

$$\frac{\|\mathbf{U}_k\|_F^2 + \|\mathbf{V}_k\|_F^2}{2|\langle \mathbf{U}_k, \mathbf{V}_k \rangle|} \geq 1. \quad (18)$$

The relation in (18) motivates us to use the following *adaptive* strategy for updating λ :

$$\lambda_{k+1} = \lambda_k \cdot \frac{\|\mathbf{U}_k\|_F^2 + \|\mathbf{V}_k\|_F^2}{2|\langle \mathbf{U}_k, \mathbf{V}_k \rangle|}, \quad k \geq 0, \quad (19)$$

where the initial regularization parameter $\lambda_0 > 0$ can be selected as a very small number, e.g., $\lambda_0 = 10^{-5}$. Note that \mathbf{U}_k and \mathbf{V}_k will not tend to be orthogonal as we are minimizing $\|\mathbf{U} - \mathbf{V}\|_F^2$. Therefore, the formula (19) is well defined as the denominator is bounded away from zero as the iteration proceeds.

To understand this adaptive strategy, we note that by (18), the parameter λ_k keeps increasing at each iteration until

$$\frac{\|\mathbf{U}_k\|_F^2 + \|\mathbf{V}_k\|_F^2}{2|\langle \mathbf{U}_k, \mathbf{V}_k \rangle|} = 1.$$

The above happens only when² $\mathbf{U}_k = \mathbf{V}_k$, which indeed is the goal we want to achieve. On the one hand, the two

2. It can also happen when $\mathbf{U}_k = -\mathbf{V}_k$, but since the algorithm minimizes $\|\mathbf{U} - \mathbf{V}\|_F^2$, this case in practice is likely impossible.

factors can reach consensus without requiring λ_k to go to infinitely large, as guaranteed by Theorem 3. On the other hand, we note that the algorithm may already converge and $\mathbf{U}^* = \mathbf{V}^*$ even with $\lambda_k \leq \bar{\lambda}$, where $\bar{\lambda}$ is the lower bound in (17). There is no contradiction to Theorem 3 as (17) is a sufficient but not necessary condition to guarantee convergence and consensus. In fact, this is one of the advantages of using this adaptive strategy since a smaller penalty term can allow the algorithms focus more on the data fidelity term. We refer to Figure 1 in next Section for an illustration of the practical performance of the adaptive strategy (19).

It is worth mentioning that our idea of updating the penalty parameter λ has the potential to be used widely in other Augmented Lagrangian-based algorithms and splitting algorithms since these type of methods usually use squared Euclidean distance to penalize violation of the constraints.

4 NUMERICAL EXPERIMENTS

In this section, we conduct experiments on both synthetic data and real image clustering to illustrate the performance of our proposed algorithms and compare it with other state-of-the-art ones, in terms of both convergence property and clustering accuracy.

For comparison in terms of solving the original symmetric NMF (2), we define

$$E^k = \frac{\|\mathbf{X} - \mathbf{U}_k(\mathbf{U}_k)^T\|_F^2}{\|\mathbf{X}\|_F^2}$$

as the normalized fitting error at the k -th iteration.

Besides SymANLS, SymHALS and A-SymHALS for which we set the inner iteration number $L = 2$ in Algorithm 3, we list several state-of-the-art algorithms to compare: 1) ADMM [28], which solves an equality constrained nonsymmetric NMF using a primal dual method; 2) truncated SVD (tSVD) [26], which utilizes SVD to iteratively approximate the solution to the original symmetric NMF (2); 3) beta Symmetric Nonnegative Matrix Factorization (**beta-SNMF**) [17], which is an accelerated version of the well-known multiplicative update algorithm in NMF literature; 4) PGD [13].

4.1 Experiments with Synthetic Data

We randomly generate a matrix $\mathbf{U} \in \mathbb{R}^{n \times r}$ with each entry independently following a standard Gaussian distribution. To enforce nonnegativity, we then take absolute value on each entry of \mathbf{U} to get \mathbf{U}^* . Data matrix \mathbf{X} is constructed as $\mathbf{X} = \mathbf{U}^* \mathbf{U}^{*T} + \sigma|\mathbf{N}|$, where \mathbf{N} represents the noise and σ is the noise level. Unless explicitly specified, each entry of the noisy matrix \mathbf{N} follows an *i.i.d.* standard Gaussian distribution. We initialize all algorithms with \mathbf{U}_0 , whose entries are *i.i.d.* uniformly distributed between 0 and 1.

We first verify the adaptive formula (19) for updating the parameter λ . Figure 1 displays the penalty term $\|\mathbf{U}_k - \mathbf{V}_k\|_F^2$ and the penalty parameter λ_k updated using (19) versus iteration count k . One can observe that the term $\|\mathbf{U}_k - \mathbf{V}_k\|_F^2$ converges to 0 and λ_k converges to a finite value for our proposed algorithms. In the sequel, we utilize (19) to update the parameter λ with $\lambda_0 = 10^{-5}$ for all experiments.

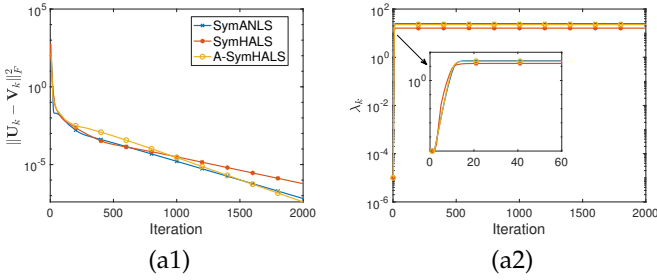


Fig. 1. (a1): The penalty term $\|U_k - V_k\|_F^2$ versus iteration number. (a2): The penalty parameter λ_k versus iteration number. Here, $\lambda_0 = 10^{-5}$, $n = 50$, $r = 5$, $\sigma = 0$.

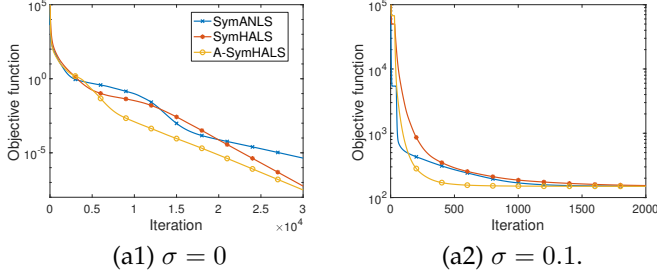


Fig. 2. Convergence of the proposed algorithms on synthetic data with different noise level σ , where $n = 300$, $r = 20$.

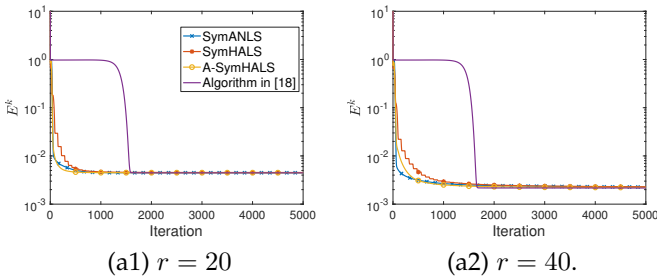


Fig. 3. Normalized fitting error E^k versus iteration number on synthetic data with $n = 300$, $\sigma = 0.1$, and varied factorization rank r .

We now verify the convergence behaviors of our proposed algorithms when utilized to solve problem (3) and display the result in Figure 2. One can observe that our algorithms converge in both noise-free ($\sigma = 0$) and noisy ($\sigma = 0.1$) cases, which corroborates our theoretical results. It is also worth noting that A-SymHALS converges slightly faster than SymHALS, which supports the acceleration technique used in A-SymHALS. Interestingly, in the noise-free case, all the three proposed algorithms have a linear rate of convergence and can find a nearly globally optimal minimizer of problem (3) (asserted by achieving nearly zero function value) even if the problem is nonconvex.

As mentioned in Section 1.2, the idea of solving symmetric NMF by the penalized nonsymmetric NMF (3) has also appeared heuristically in [18]. The authors proposed to solve problem (3) using an ANLS-type method, where the penalty parameter λ is updated as $\lambda_{k+1} = 1.01 \times \lambda_k$ until $\|U_k - V_k\|_F / \|V_k\|_F < 10^{-8}$. Thus, their algorithm is the same as our SymANLS except for the updating of the penalty parameter λ . In Figure 3, we compare our proposed algorithms with theirs in terms of the normalized fitting

error E^k . Though they all eventually converge to the same E_k , our algorithms converge much faster than theirs. The relatively slow convergence of their algorithm is due to the fact that their updating of the penalty parameter λ is not adaptive to the iterations of the algorithm. Using Figure 3 (a1) as an example, λ_k in our algorithms is increased to around 97 after only 85 iterations and then remains this value for the following iterations (i.e., the adaptive updating formula (19) nearly converges after 85 iterations), while their algorithm needs 1619 iterations to update λ_k to around 97 and keeps increasing λ_k to 7×10^7 after 3000 iterations. Increasing the penalty parameter to infinity is a common strategy utilized in the analysis of methods of Lagrangian multipliers for general problems [21, Theorem 17.1]. We avoid such a requirement by exploiting the specific structures within problem (3). Thus, it is instructive to emphasize that the difference between our work and [18] does not only lie in the update of the penalty parameter λ , but also on the theoretical side; see Section 1.1 and 1.2 for more details. In the sequel, we will not display the performance of the algorithm in [18] since it has very similar performance to our SymANLS except for relatively slower convergence.

In Figure 4, we compare our algorithms with several state-of-the-art symmetric NMF algorithms by displaying the normalized fitting error E^k versus iteration number and wall clock running time, which demonstrates the ability for solving the original symmetric NMF (2). We fix $n = 300$ and vary the factorization rank r and the noise level σ . From the top row of Figure 4 (i.e., Figure 4 (a1)-(a4)), it can be observed that our proposed SymANLS, SymHALS, and A-SymHALS outperform the others in terms of iteration number. A-SymHALS performs the best in the noise free settings, while SymANLS, SymHALS, and A-SymHALS have comparable performances in the noisy cases. The bottom row of Figure 4 (i.e., Figure 4 (b1)-(b4)) demonstrates the evolution of E^k versus wall clock running time. It can be observed that SymHALS and A-SymHALS have the best performances among other algorithms. In Figure 4 (b1), where the factorization rank is small ($r = 20$) and the data is not contaminated by noise, the tSVD algorithm also performs well. However, when noise is presented and the factorization rank r becomes larger, SymHALS and A-SymHALS have the best running time performance. On the other hand, one can observe from the experiments where noise is added (i.e., (a2), (b2), (a4), (b4)), the alternating-type algorithms, ADMM, and PGD can converge to solutions with almost the same fitting error E^k after enough iterations, while tSVD and beta-SNMF likely get stuck at local minima with larger fitting errors.

To further investigate the performance of our proposed algorithms, we vary several experimental parameters and show the results in Figure 5. We run each algorithm 3×10^4 iterations for each parameter setting in order to ensure convergence. In Figure 5 (a1), we fix $r = 20$, $\sigma = 0.1$ and vary $n \in \{100, 150, 200, 250, 300, 350, 400\}$. It is observed that varying n while keeping the other parameters fixed does not affect too much the performance of each algorithm. This is reasonable as varying n has almost no effect to the signal-to-noise ratio. We can conclude from Figure 5 (a1) that our algorithms and ADMM outperform others for different n . In Figure 5 (a2), we fix $n = 300$, $\sigma = 0.1$ and vary

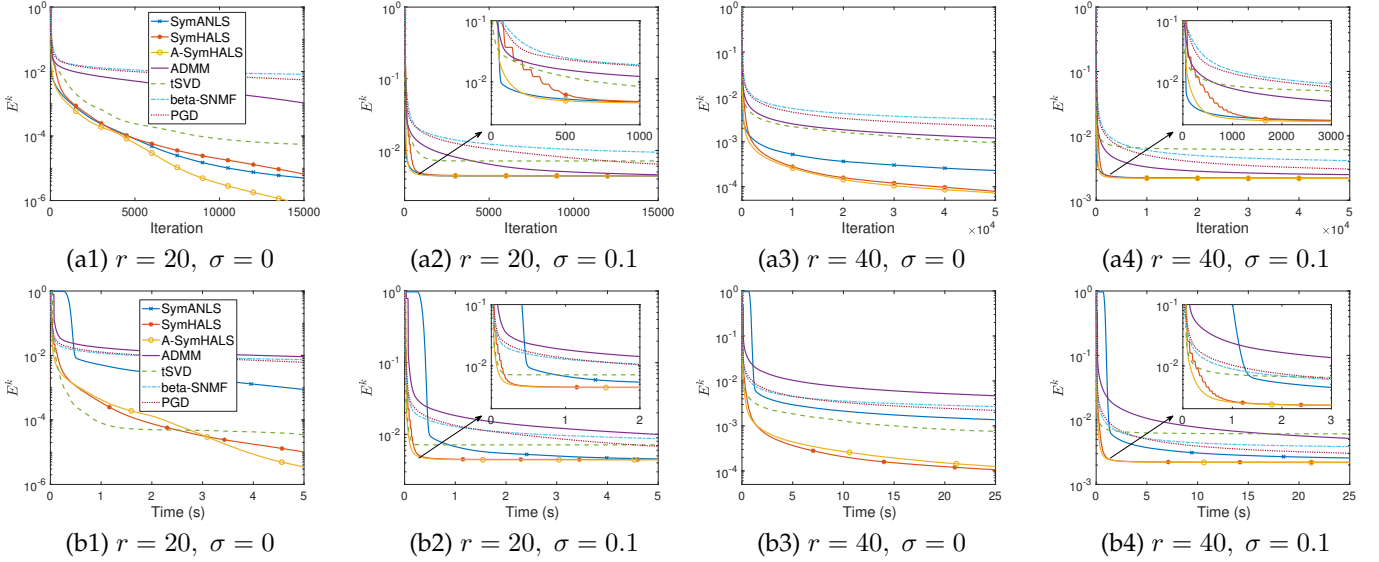


Fig. 4. Normalized fitting error E^k versus iteration number (top row) and wall clock running time (bottom row) on synthetic data with $n = 300$, varied factorization rank r and noise level σ .

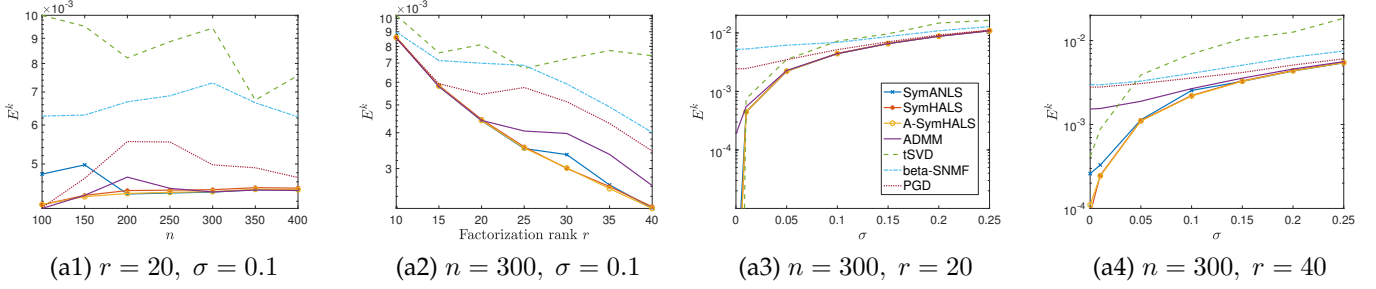


Fig. 5. Normalized fitting error E^k on synthetic data by varying experimental parameters. (a1): data size $n \in \{100, 150, 200, 250, 300, 350, 400\}$. (a2): Factorization rank $r \in \{10, 15, 20, 25, 30, 35, 40\}$. (a3): Noise level $\sigma \in \{0, 0.01, 0.05, 0.1, 0.15, 0.2, 0.25\}$. (a4): Noise level $\sigma \in \{0, 0.01, 0.05, 0.1, 0.15, 0.2, 0.25\}$.

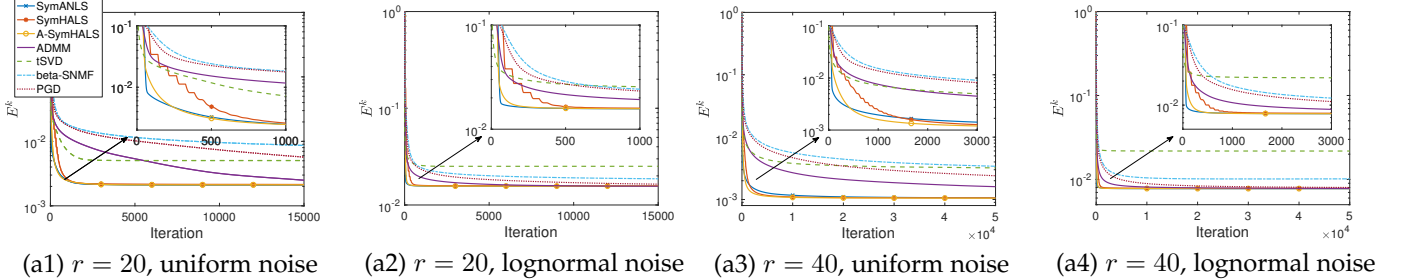


Fig. 6. Normalized fitting error E^k versus iteration number on synthetic data with $n = 300$, noise level $\sigma = 0.1$, varied factorization rank r , and varied noise distributions.

$r \in \{10, 15, 20, 25, 30, 35, 40\}$. It is clear that our algorithms outperform others for almost all choices of r . We also vary the noise level $\sigma \in \{0, 0.01, 0.05, 0.1, 0.15, 0.2, 0.25\}$ in Figure 5 (a3) (where $n = 300$, $r = 20$) and Figure 5 (a4) (where $n = 300$, $r = 40$). We observe that our algorithms perform better than others for almost all choices of σ .

From Figure 4 and 5, we can observe the robustness of our proposed algorithms to Gaussian noise. We further exam the performance on other types of noise. With the same experimental settings as used to generate Figure 4 (except for the noise distribution), we test all algorithms on synthetic data contaminated by noise generated according

to the uniform distribution and the lognormal distribution; see Figure 6. We can observe similar phenomena that our proposed algorithms perform better than others in these cases.

4.2 Image Clustering

Symmetric NMF can be used for graph clustering where each element X_{ij} denotes the similarity between data i and j [16], [18]. In this subsection, we apply different symmetric NMF algorithms for graph clustering on real image datasets

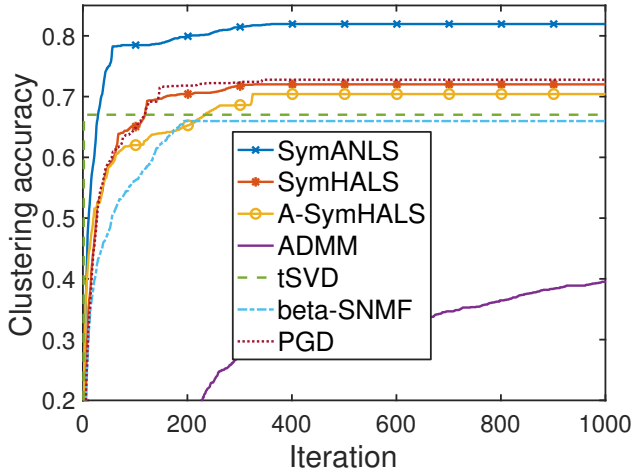
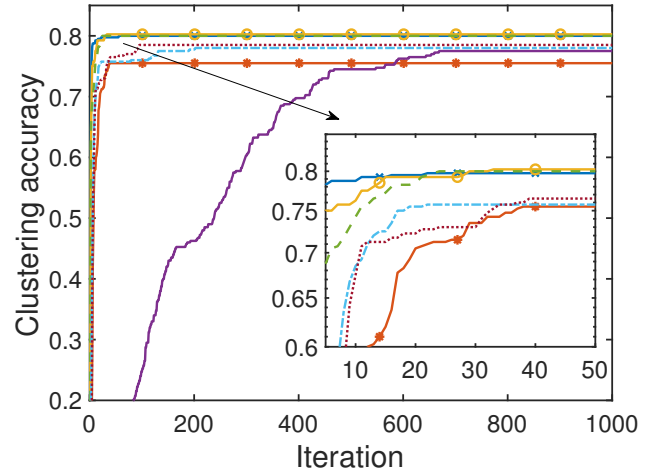
(a1) COIL-20 dataset, $n = 1440$, $r = 20$ (a2) ORL dataset, $n = 400$, $r = 40$.

Fig. 7. Image clustering accuracy versus iteration number on real dataset.

TABLE 1
Summary of image clustering accuracy of different algorithms on five image datasets

	ORL	COIL-20	MNIST _{train}	TDT2	MNIST _{test}
SymANLS	0.8000	0.8194	0.6217	0.9793	0.8589
SymHALS	0.7550	0.7201	0.6393	0.9800	0.8589
A-SymHALS	0.8025	0.7042	0.7043	0.9803	0.8589
ADMM	0.7750	0.6937	0.5803	0.9800	0.8713
tSVD	0.8000	0.6701	0.6653	0.6044	0.9050
beta-SNMF	0.7800	0.6597	0.5100	0.9647	0.8513
PGD	0.7850	0.7278	0.6287	0.8313	0.9136

and compare the clustering accuracy [33].³

We first put all images to be clustered in a data matrix \mathbf{M} , where each row is a vectorized image. We then construct the similarity matrix following the procedures in [18, section 7.1, step 1 to step 3], and utilize self-tuning method to form the similarity matrix \mathbf{X} . Upon deriving $\tilde{\mathbf{U}}$ from symmetric NMF $\mathbf{X} \approx \tilde{\mathbf{U}}\tilde{\mathbf{U}}^T$, the label of the i -th image can be obtained by:

$$\text{label}(\mathbf{M}_i) = \arg \max_j \tilde{\mathbf{U}}_{(ij)}. \quad (20)$$

We conduct the experiments on four image datasets:

ORL: 400 facial images from 40 different persons with each one having 10 images from different angles and emotions⁴.

COIL-20: 1440 images from 20 objects⁵.

TDT2: 10,212 news articles from 30 categories⁶. We extract the first 3147 data for experiments (containing only 2 categories).

MNIST: classical handwritten digits dataset⁷, from

3. Note that there exist many other clustering methods, but comparing with them is not the focus of this paper. Instead, we only compare different symmetric NMF algorithms to demonstrate the performance of the proposed algorithms for solving symmetric NMF.

4. <http://www.cl.cam.ac.uk/research/dtg/attarchive/facedatabase>

5. <http://www.cs.columbia.edu/CAVE/software/softlib/coil-20.php>

6. <https://www ldc.upenn.edu/collaborations/past-projects>

7. <http://yann.lecun.com/exdb/mnist/>

which we take the first 3147 images from each of the training and test sets.

In Figure 7 (a1), we display the clustering accuracy on dataset **COIL-20** versus iteration number. Similar results for dataset **ORL** are plotted in Figure 7 (a2). We observe that though tSVD and beta-SNMF have fast convergence speed, they often provide worse clustering accuracies compared to the proposed methods, which is consistent with the conclusion drawn in the noisy synthetic experiments. We note that the performance of ADMM will increase as iteration goes and after almost 6000 iterations it reaches a comparable result to other algorithms on COIL-20 dataset. Moreover, it requires more iterations for larger dataset. This observation makes ADMM less favorable for image clustering due to its computational burden. These results as well as the experimental results shown in the last subsection demonstrate (i) the power of transferring the symmetric NMF (2) to a penalized nonsymmetric one (3); and (ii) the efficiency of alternating-type algorithms for solving (3) by exploiting the splitting property within the optimization variables in (3).

Finally, Table 1 shows the clustering accuracies of the algorithms on different datasets, where we run enough iterations for ADMM so that it obtains its best results. We observe from Table 1 that SymANLS, SymHALS and A-SymHALS perform better than or have comparable performance to the others in most of the cases.

5 PROOF OF THEOREM 3

Since both SymANLS and SymHALS can be viewed as special cases of A-SymHALS in terms of convergence, we will only focus on the proof of the convergence for A-SymHALS. According to Theorem 2, the remaining task is to establish the descent property as well as the convergence behavior of A-SymHALS to a critical point of the penalized nonsymmetric NMF (3). As stated in Remark 4, the multiple update scheme in A-SymHALS destroys the possibility to directly apply the disciplined KL convergence analysis framework. Due to the multiple update scheme, we can only obtain a weaker version of the so-called safeguard property

in the standard framework (see Lemma 6), but a slightly strengthened sufficient decrease property (see Lemma 2).

5.1 Notations Used in The Proof

We stack \mathbf{U} and \mathbf{V} into one variable $\mathbf{W} := (\mathbf{U}, \mathbf{V})$. We may constantly change between the notations \mathbf{W} and (\mathbf{U}, \mathbf{V}) . Let $\mathbf{W}_k^j = (\mathbf{U}_k^j, \mathbf{V}_k^j)$ represent the j -th inner iterate generated by A-SymHALS during the update from $\mathbf{W}_k = (\mathbf{U}_k, \mathbf{V}_k)$ to $\mathbf{W}_{k+1} = (\mathbf{U}_{k+1}, \mathbf{V}_{k+1})$, with $\mathbf{W}_k^0 = \mathbf{W}_k$ and $\mathbf{W}_k^L = \mathbf{W}_{k+1}$. We designate $\mathbf{u}_{i,k}^j$ and $\mathbf{v}_{i,k}^j$ the i -th columns of \mathbf{U}_k^j and \mathbf{V}_k^j , respectively. Correspondingly, $\mathbf{u}_{i,k}$ and $\mathbf{v}_{i,k}$ represent the i -th columns of \mathbf{U}_k and \mathbf{V}_k , respectively. At the k -th outer iteration and $j+1$ -th inner iteration of \mathbf{u}_i , we denote

$$g_{i,k}^{j+1}(\mathbf{u}_i) = g(\mathbf{u}_{1,k}^{j+1}, \dots, \mathbf{u}_{i-1,k}^{j+1}, \mathbf{u}_i, \mathbf{u}_{i+1,k}^j, \dots, \mathbf{u}_{r,k}^j, \mathbf{V}_k)$$

as the function g when restricted to block \mathbf{u}_i . We will also rewrite (3) as a unconstrained optimization problem by using the function

$$f(\mathbf{U}, \mathbf{V}) = g(\mathbf{U}, \mathbf{V}) + \sigma_+(\mathbf{U}) + \sigma_+(\mathbf{V}),$$

with σ_+ being the indicator function of the nonnegative constraint.

5.2 Definitions and Basic Ingredients

Before going to the main proof, we first introduce some supporting materials.

Definition 1 (first order optimality). *A point $\mathbf{W}^* = (\mathbf{U}^*, \mathbf{V}^*)$ is called a critical point of problem (3) if it satisfies*

$$0 \in \partial f(\mathbf{W}^*) = (\nabla_{\mathbf{U}} g(\mathbf{U}^*, \mathbf{V}^*), \nabla_{\mathbf{V}} g(\mathbf{U}^*, \mathbf{V}^*) + (\partial \sigma_+(\mathbf{U}^*), \partial \sigma_+(\mathbf{V}^*)),$$

where $\partial \sigma_+$ represents the usual convex subdifferential; i.e., $\partial \sigma_+(\mathbf{U}) := \{\mathbf{S} \in \mathbb{R}^{n \times r} : \langle \mathbf{S}, \mathbf{U}' - \mathbf{U} \rangle \leq 0, \forall \mathbf{U}' \in \mathbb{R}^{n \times r}\}$.

The following property states the geometry of a function h around its critical points, which plays a key role in our sequel analysis.

Definition 2 (KL property). [32], [34] *We say a proper semi-continuous function $h(\mathbf{u})$ satisfies Kurdyka-Lojasiewicz (KL) property if for every critical point $\bar{\mathbf{u}}$ of $h(\mathbf{u})$, there exist $\delta > 0$, $\eta > 0$, $\theta \in [0, 1)$, $C_1 > 0$ such that for all*

$$\mathbf{u} \in B(\bar{\mathbf{u}}, \delta) \cap \{\mathbf{u} : h(\bar{\mathbf{u}}) < h(\mathbf{u}) < h(\bar{\mathbf{u}}) + \eta\},$$

one has

$$|h(\mathbf{u}) - h(\bar{\mathbf{u}})|^\theta \leq C_1 \text{dist}(\mathbf{0}, \partial h(\mathbf{u})),$$

where $B(\bar{\mathbf{u}}, \delta) := \{\mathbf{u} : \|\mathbf{u} - \bar{\mathbf{u}}\|_2 \leq \delta\}$.

The above KL property (also known as KL inequality) states the regularity of h around its critical point $\bar{\mathbf{u}}$. [24, Section 4] shows that our function of interest f satisfies this property. Indeed, the KL property is general enough such that a large class of functions hold such a property, including but never limited to any polynomial, any norm, any quasi norm, ℓ_0 -norm, indicator function of smooth manifold, etc; see [24], [35] for more discussions and examples.

5.3 Supporting Results

Compared with the standard sufficient decrease property of descent algorithms [23], [24], the following lemma states the strengthened sufficient decrease property of A-SymHALS.

Lemma 2. *For any $k \geq 0$, we have*

$$\begin{aligned} & f(\mathbf{W}_k) - f(\mathbf{W}_{k+1}) \\ & \geq \frac{\lambda}{4L} \left[\|\mathbf{W}_{k+1} - \mathbf{W}_k\|_F^2 + \sum_{j=0}^{L-1} \|\mathbf{W}_k^{j+1} - \mathbf{W}_k^j\|_F^2 \right]. \end{aligned} \quad (21)$$

Proof of Lemma 2. In the $j+1$ -th inner iteration for updating \mathbf{U}_k to \mathbf{U}_{k+1} , suppose we update \mathbf{u}_i , which amounts to solve the subproblem (see Section 5.1 about notations)

$$\min_{\mathbf{u}_i} f_{i,k}^{j+1}(\mathbf{u}_i) = g_{i,k}^{j+1}(\mathbf{u}_i) + \sigma_+(\mathbf{u}_i).$$

Since $f_{i,k}^{j+1}(\mathbf{u}_i)$ is λ -strongly convex due to the penalty term $\frac{\lambda}{2} \|\mathbf{u}_i - \mathbf{v}_{i,k}\|_2^2$ of $g_{i,k}^{j+1}$, we have

$$f_{i,k}^{j+1}(\mathbf{x}) \geq f_{i,k}^{j+1}(\mathbf{y}) + \langle \mathbf{s}, \mathbf{x} - \mathbf{y} \rangle + \frac{\lambda}{2} \|\mathbf{x} - \mathbf{y}\|_2^2,$$

for all $\mathbf{x}, \mathbf{y} \in \mathbb{R}^{n \times 1}$ and $\mathbf{s} \in \partial_{\mathbf{u}_i} f_{i,k}^{j+1}(\mathbf{y})$. Substituting $\mathbf{x} = \mathbf{u}_{i,k}^j$ and $\mathbf{y} = \mathbf{u}_{i,k}^{j+1}$ yields

$$f_{i,k}^{j+1}(\mathbf{u}_{i,k}^j) \geq f_{i,k}^{j+1}(\mathbf{u}_{i,k}^{j+1}) + \frac{\lambda}{2} \|\mathbf{u}_{i,k}^j - \mathbf{u}_{i,k}^{j+1}\|_2^2,$$

where we also used the optimality of $\mathbf{u}_{i,k}^{j+1}$ in the subproblem which implies that $0 \in \partial_{\mathbf{u}_i} f_{i,k}^{j+1}(\mathbf{u}_{i,k}^{j+1})$. Upon summing both sides of the above inequality over $i = 1, \dots, r$, one has

$$f(\mathbf{U}_k^j, \mathbf{V}_k) - f(\mathbf{U}_k^{j+1}, \mathbf{V}_k) \geq \frac{\lambda}{2} \|\mathbf{U}_k^{j+1} - \mathbf{U}_k^j\|_F^2,$$

for all $j \in \{0, 1, \dots, L-1\}$. Summing both sides of the above inequalities for j from 0 to $L-1$ gives

$$\begin{aligned} f(\mathbf{U}_k, \mathbf{V}_k) - f(\mathbf{U}_{k+1}, \mathbf{V}_k) &= \sum_{j=0}^{L-1} f(\mathbf{U}_k^j, \mathbf{V}_k) - f(\mathbf{U}_k^{j+1}, \mathbf{V}_k) \\ &\geq \frac{\lambda}{4} \sum_{j=0}^{L-1} \|\mathbf{U}_k^{j+1} - \mathbf{U}_k^j\|_F^2 + \frac{\lambda}{4} \sum_{j=0}^{L-1} \|\mathbf{U}_k^{j+1} - \mathbf{U}_k^j\|_F^2 \\ &\stackrel{(i)}{\geq} \frac{\lambda}{4} \frac{\left(\|\mathbf{U}_k^1 - \mathbf{U}_k^0\|_F + \dots + \|\mathbf{U}_k^L - \mathbf{U}_k^{L-1}\|_F \right)^2}{L} \\ &\quad + \frac{\lambda}{4} \sum_{j=0}^{L-1} \|\mathbf{U}_k^{j+1} - \mathbf{U}_k^j\|_F^2 \\ &\stackrel{(ii)}{\geq} \frac{\lambda}{4L} \|\mathbf{U}_{k+1} - \mathbf{U}_k\|_F^2 + \frac{\lambda}{4} \sum_{j=0}^{L-1} \|\mathbf{U}_k^{j+1} - \mathbf{U}_k^j\|_F^2. \end{aligned}$$

where (i) used the fact that $\sqrt{\frac{a_1^2 + a_2^2 + \dots + a_L^2}{L}} \geq \frac{|a_1| + |a_2| + \dots + |a_L|}{L}$, and (ii) follows from the triangle inequality. We complete the proof by using a similar argument to obtain

$$\begin{aligned} & f(\mathbf{U}_{k+1}, \mathbf{V}_k) - f(\mathbf{U}_{k+1}, \mathbf{V}_{k+1}) \\ & \geq \frac{\lambda}{4L} \|\mathbf{V}_{k+1} - \mathbf{V}_k\|_F^2 + \frac{\lambda}{4} \sum_{j=0}^{L-1} \|\mathbf{V}_k^{j+1} - \mathbf{V}_k^j\|_F^2. \end{aligned}$$

The desired result can be obtained by summing up the above two inequalities. \square

Lemma 2 has the following direct result, which states the descent property of A-SymHALS. This fulfills the requirement of decreasing the objective function in Theorem 2.

Lemma 3. For any $k \geq 0$, we have:

- (a) *The sequence $\{f(\mathbf{U}_k, \mathbf{V}_k)\}_{k \geq 0}$ of function values is monotonically decreasing and it converges to some finite value $f^* \geq 0$:*

$$\lim_{k \rightarrow \infty} f(\mathbf{U}_k, \mathbf{V}_k) = f^*.$$

- (b) *The sequence $\{f(\mathbf{U}_k, \mathbf{V}_k)\}_{k \geq 0}$ is regular, i.e.,*

$$\lim_{k \rightarrow \infty} \|\mathbf{U}_{k+1} - \mathbf{U}_k\|_F = 0, \quad \lim_{k \rightarrow \infty} \|\mathbf{V}_{k+1} - \mathbf{V}_k\|_F = 0. \quad (22)$$

Lemma 2 together with Lemma 1 also implies the boundedness of the sequence $\{(\mathbf{W}_k)\}_{k \geq 0} = \{(\mathbf{U}_k, \mathbf{V}_k)\}_{k \geq 0}$.

Lemma 4. The sequence $\{(\mathbf{W}_k)\}_{k \geq 0} = \{(\mathbf{U}_k, \mathbf{V}_k)\}_{k \geq 0}$ lies in a bounded subset.

The following lemma estimates the local Lipschitz constant of the gradient of function g in (3).

Lemma 5. The function $g(\mathbf{U}, \mathbf{V}) = \frac{1}{2}\|\mathbf{X} - \mathbf{U}\mathbf{V}^T\|_F^2 + \frac{\lambda}{2}\|\mathbf{U} - \mathbf{V}\|_F^2$ in (3) has Lipschitz continuous gradient with the Lipschitz constant as $2B + \lambda + \|\mathbf{X}\|_F$ in any bounded ℓ_2 -norm ball $\{(\mathbf{U}, \mathbf{V}) : \|\mathbf{U}\|_F^2 + \|\mathbf{V}\|_F^2 \leq B\}$ for any $B > 0$.

Proof. To obtain the Lipschitz constant, it is equivalent to bound the spectral norm of the quadrature form of the Hessian $[\nabla^2 g(\mathbf{W})](\mathbf{D}, \mathbf{D})$ for any $\mathbf{D} := (\mathbf{D}_U, \mathbf{D}_V)$:

$$\begin{aligned} & [\nabla^2 g(\mathbf{W})](\mathbf{D}, \mathbf{D}) \\ &= \|\mathbf{U}\mathbf{D}_V^T + \mathbf{D}_U\mathbf{V}^T\|_F^2 - 2\langle \mathbf{X}, \mathbf{D}_U\mathbf{D}_V^T \rangle + \frac{\lambda}{2}\|\mathbf{D}_V - \mathbf{D}_U\|_F^2 \\ &\leq 2\|\mathbf{U}\|_F^2\|\mathbf{D}_V\|_F^2 + 2\|\mathbf{V}\|_F^2\|\mathbf{D}_U\|_F^2 \\ &\quad + \underbrace{\lambda\|\mathbf{D}_U\|_F^2 + \lambda\|\mathbf{D}_V\|_F^2}_{=\lambda\|\mathbf{D}\|_F^2} + 2\|\mathbf{X}\|_F \underbrace{\|\mathbf{D}_U\mathbf{D}_V^T\|_F}_{\leq \|\mathbf{D}\|_F^2/2} \\ &\leq (2\|\mathbf{U}\|_F^2 + 2\|\mathbf{V}\|_F^2 + \lambda + \|\mathbf{X}\|_F)\|\mathbf{D}\|_F^2 \\ &\leq (2B + \lambda + \|\mathbf{X}\|_F)\|\mathbf{D}\|_F^2. \end{aligned}$$

\square

As the iterate $\mathbf{W}_k = (\mathbf{U}_k, \mathbf{V}_k)$ for all $k \geq 0$ lives in the ℓ_2 -norm ball with the radius $\sqrt{B_0}$ (see (12) for definition of B_0) according to Lemma 1 and Lemma 3, the function g has Lipschitz continuous gradient with the Lipschitz constant being $2B_0 + \lambda + \|\mathbf{X}\|_F$ around each \mathbf{W}_k .

Lemma 6. For any $k \geq 0$, we have

$$\begin{aligned} & \text{dist}(\mathbf{0}, \partial f(\mathbf{U}_{k+1}, \mathbf{V}_{k+1})) \\ & \leq 2r(2B_0 + \lambda + \|\mathbf{X}\|_F)\|\mathbf{W}_{k+1} - \mathbf{W}_k^{L-1}\|_F. \end{aligned} \quad (23)$$

Proof of Lemma 6. The i -th block $\mathbf{u}_{i,k+1}$ of \mathbf{U}_{k+1} is updated according to

$$\mathbf{u}_{i,k+1} = \mathbf{u}_{i,k}^L = \arg \min_{\mathbf{u}} g_{i,k}^L(\mathbf{u}) + \delta_+(\mathbf{u}).$$

It then follows from the first order optimality that

$$-\nabla g_{i,k}^L(\mathbf{u}_{i,k+1}) \in \partial \delta_+(\mathbf{u}_{i,k+1}),$$

which together with

$$\partial_{\mathbf{u}_i} f(\mathbf{U}_{k+1}, \mathbf{V}_{k+1}) = \nabla_{\mathbf{u}_i} g(\mathbf{U}_{k+1}, \mathbf{V}_{k+1}) + \partial \delta_+(\mathbf{u}_{i,k+1})$$

gives

$$\nabla_{\mathbf{u}_i} g(\mathbf{U}_{k+1}, \mathbf{V}_{k+1}) - \nabla g_{i,k}^L(\mathbf{u}_{i,k+1}) \in \partial_{\mathbf{u}_i} f(\mathbf{U}_{k+1}, \mathbf{V}_{k+1}).$$

Similar result holds for $\partial_{\mathbf{v}_i} f(\mathbf{U}_{k+1}, \mathbf{V}_{k+1})$. Now invoke the Lipschitz gradient condition of function $g(\mathbf{U}, \mathbf{V})$ in Lemma 5:

$$\begin{aligned} \text{dist}(\mathbf{0}, \partial f(\mathbf{U}_{k+1}, \mathbf{V}_{k+1})) &\leq \sum_{i=1}^r \text{dist}(\mathbf{0}, \partial_{\mathbf{u}_i} f(\mathbf{U}_{k+1}, \mathbf{V}_{k+1})) \\ &\quad + \sum_{i=1}^r \text{dist}(\mathbf{0}, \partial_{\mathbf{v}_i} f(\mathbf{U}_{k+1}, \mathbf{V}_{k+1})) \\ &\leq 2r(2B_0 + \lambda + \|\mathbf{X}\|_F)\|\mathbf{W}_{k+1} - \mathbf{W}_k^{L-1}\|_F. \end{aligned}$$

\square

We denote $\mathcal{C}(\mathbf{W}_0)$ as the collection of all the limit points of the sequence $\{\mathbf{W}_k\}$ (which may depend on the initialization \mathbf{W}_0). The following lemma provides some useful properties and optimality of $\mathcal{C}(\mathbf{W}_0)$.

Lemma 7. f is constant on $\mathcal{C}(\mathbf{W}_0)$ and

$$\lim_{k \rightarrow \infty} f(\mathbf{U}_k, \mathbf{V}_k) = f(\mathbf{U}^*, \mathbf{V}^*), \quad \forall (\mathbf{U}^*, \mathbf{V}^*) \in \mathcal{C}(\mathbf{W}_0).$$

Proof of Lemma 7. According to Lemma 4, we can extract an arbitrary convergent subsequence $\{\mathbf{W}_{k_m}\}_{m \geq 0}$ which converges to $\mathbf{W}^* \in \mathcal{C}(\mathbf{W}_0)$. By the definition of the algorithm we have

$$\mathbf{U}_{k_m} \geq 0, \quad \mathbf{V}_{k_m} \geq 0, \quad \forall k_m \geq 0.$$

Thus,

$$\lim_{m \rightarrow \infty} \delta_+(\mathbf{U}_{k_m}) = 0, \quad \lim_{m \rightarrow \infty} \delta_+(\mathbf{V}_{k_m}) = 0.$$

We now take limit on the subsequence $\{\mathbf{W}_{k_m}\}_m$:

$$\lim_{m \rightarrow \infty} f(\mathbf{W}_{k_m}) = g\left(\lim_{m \rightarrow \infty} \mathbf{W}_{k_m}\right) = g(\mathbf{W}^*),$$

where we have used the continuity of the smooth part $g(\mathbf{W})$ in (3). Then from Lemma 3 we know that $\{f(\mathbf{W}_k)\}_{k \geq 0}$ forms a convergent sequence. The proof is completed by noting that for any convergent sequence, all its subsequence must converge to a unique limiting point. \square

Lemma 8. Each element of $\mathcal{C}(\mathbf{W}^0)$ is a critical point of (3) and $\mathcal{C}(\mathbf{W}^0)$ is a nonempty, compact, and connected set with

$$\lim_{k \rightarrow \infty} \text{dist}(\mathbf{W}_k, \mathcal{C}(\mathbf{W}^0)) = 0.$$

Proof of Lemma 8. Let \mathbf{S}_k and \mathbf{D}_k be defined in Lemma 6. From Lemma 3, we have $\|\mathbf{W}_{k+1} - \mathbf{W}_k\|_F \rightarrow 0$. Hence

$$\lim_{k \rightarrow \infty} (\mathbf{S}_k, \mathbf{D}_k) = \mathbf{0}.$$

According to Lemma 4, we can extract an arbitrary convergent subsequence $\{\mathbf{W}_{k_m}\}_{m \geq 0}$ with limit \mathbf{W}^* . Note that

$$\mathbf{S}_{k_m} = \nabla_{\mathbf{U}} g(\mathbf{U}_{k_m}, \mathbf{V}_{k_m}) + \overline{\mathbf{S}}_{k_m}, \quad \overline{\mathbf{S}}_{k_m} \in \partial \delta_+(\mathbf{U}_{k_m}).$$

Since $\lim_{m \rightarrow \infty} \mathbf{S}_{k_m} = \mathbf{0}$, $\lim_{m \rightarrow \infty} \mathbf{W}_{k_m} = \mathbf{W}^*$, and $\nabla_{\mathbf{U}} g$ is continuous, $\{\overline{\mathbf{S}}_{k_m}\}$ is convergent. Denote by $\overline{\mathbf{S}}^* =$

$\lim_{m \rightarrow \infty} \bar{\mathbf{S}}_{k_m}$. By the definition of $\bar{\mathbf{S}}_{k_m} \in \partial \delta_+(\mathbf{U}_{k_m})$, for any $\mathbf{U}' \in \mathbb{R}^{n \times r}$, we have

$$\delta_+(\mathbf{U}') - \delta_+(\mathbf{U}_{k_m}) \geq \langle \bar{\mathbf{S}}_{k_m}, \mathbf{U}' - \mathbf{U}_{k_m} \rangle.$$

Due to $\lim_{m \rightarrow \infty} \delta_+(\mathbf{U}_{k_m}) = 0 = \delta_+(\mathbf{U}^*)$ (since $\mathbf{U}_{k_m} \geq 0$), taking $m \rightarrow \infty$ for both sides of the above equation gives

$$\delta_+(\mathbf{U}') - \delta_+(\mathbf{U}^*) \geq \langle \bar{\mathbf{S}}^*, \mathbf{U}' - \mathbf{U}^* \rangle.$$

As the above equation holds for any $\mathbf{U}' \in \mathbb{R}^{n \times r}$, we have $\bar{\mathbf{S}}^* \in \partial \delta_+(\mathbf{U}^*)$ and $\mathbf{0} = \nabla_{\mathbf{U}} g(\mathbf{U}^*, \mathbf{V}^*) + \bar{\mathbf{S}}^* \in \partial_{\mathbf{U}} f(\mathbf{W}^*)$. With similar argument, we get $\mathbf{0} \in \partial_{\mathbf{V}} f(\mathbf{W}^*)$ and thus

$$\mathbf{0} \in \partial f(\mathbf{W}^*),$$

which implies that \mathbf{W}^* is a critical point of (3).

Finally, by [24, Lemma 5] and identifying that the sequence $\{\mathbf{W}_k\}$ is bounded and regular (i.e. $\lim_{k \rightarrow \infty} \|\mathbf{W}_{k+1} - \mathbf{W}_k\|_F = 0$), we conclude that the set of limit points $\mathcal{C}(\mathbf{W}_0)$ is a nonempty, compact, and connect set satisfying

$$\lim_{k \rightarrow \infty} \text{dist}(\mathbf{W}_k, \mathcal{C}(\mathbf{W}_0)) = 0.$$

□

With the KL property of f (see Definition 2), Lemma 7, and Lemma 8, we have the following *uniform* KL property of f on the set $\mathcal{C}(\mathbf{W}_0)$ by following the argument of [24, Lemma 6].

Lemma 9. *There exist a set of uniform constants $C_2 > 0$, $\delta > 0$, $\eta > 0$ and $\theta \in [0, 1)$ such that for all $\mathbf{W}^* \in \mathcal{C}(\mathbf{W}_0)$ and \mathbf{W} in the following intersection*

$$B(\mathcal{C}(\mathbf{W}_0), \delta) \cap \{\mathbf{W} : f(\mathbf{W}^*) < f(\mathbf{W}) < f(\mathbf{W}^*) + \eta\},$$

we have

$$|f(\mathbf{W}) - f(\mathbf{W}^*)|^\theta \leq C_2 \text{dist}(\mathbf{0}, \partial f(\mathbf{W})).$$

5.4 Formal Proof of Theorem 3

Proof of Theorem 3. With all the intermediate techniques developed above, we are now going to complete the proof of Theorem 3; that is, showing that the sequence of iterates $\{\mathbf{W}_k\}_{k \geq 0}$ generated by A-SymHALS is convergent and converges to a critical point \mathbf{W}^* of (3).

Recall Lemma 8 that $\lim_{k \rightarrow \infty} \text{dist}(\mathbf{W}_k, \mathcal{C}(\mathbf{W}_0)) = 0$ and Lemma 7 that $\lim_{k \rightarrow \infty} f(\mathbf{W}_k) = f(\mathbf{W}^*)$, $\forall \mathbf{W}^* \in \mathcal{C}(\mathbf{W}_0)$. For any fixed $\delta > 0, \eta > 0$, there exists $k_0 > 0$ such that $\text{dist}(\mathbf{W}_k, \mathcal{C}(\mathbf{W}_0)) \leq \delta$ and $f(\mathbf{W}_k) < f(\mathbf{W}^*) + \eta$ for all $k \geq k_0$. Furthermore, from Lemma 3, we have $f(\mathbf{W}_k) > f(\mathbf{W}^*)$ for all $k \geq 0$. Hence, from Lemma 9 one has

$$[f(\mathbf{W}_k) - f(\mathbf{W}^*)]^\theta \leq C_3 \text{dist}(\mathbf{0}, \partial f(\mathbf{W}_k)) \quad \forall k \geq k_0. \quad (24)$$

In the subsequent analysis, we restrict to $k \geq k_0$. Construct a concave function $x^{1-\theta}$ for some $\theta \in [0, 1)$ with domain $x > 0$. Obviously, by the concavity, we have

$$x_2^{1-\theta} - x_1^{1-\theta} \geq (1-\theta)x_2^{-\theta}(x_2 - x_1), \quad \forall x_1 > 0, x_2 > 0.$$

By replacing x_1 by $f(\mathbf{W}_{k+1}) - f(\mathbf{W}^*)$ and x_2 by $f(\mathbf{W}_k) - f(\mathbf{W}^*)$ and using the sufficient decrease property in

Lemma 2, we have (we will hide all absolute and independent constants in \bar{C} to simplify notation)

$$\begin{aligned} & (f(\mathbf{W}_k) - f(\mathbf{W}^*))^{1-\theta} - (f(\mathbf{W}_{k+1}) - f(\mathbf{W}^*))^{1-\theta} \\ & \geq \bar{C} \frac{f(\mathbf{W}_k) - f(\mathbf{W}_{k+1})}{(f(\mathbf{W}_k) - f(\mathbf{W}^*))^\theta} \\ & \geq \bar{C} \frac{\|\mathbf{W}_{k+1} - \mathbf{W}_k\|_F^2 + \sum_{j=0}^{L-1} \|\mathbf{W}_k^{j+1} - \mathbf{W}_k^j\|_F^2}{\text{dist}(\mathbf{0}, \partial f(\mathbf{W}_k))} \\ & \geq \bar{C} \frac{\|\mathbf{W}_{k+1} - \mathbf{W}_k\|_F^2 + \sum_{j=0}^{L-1} \|\mathbf{W}_k^{j+1} - \mathbf{W}_k^j\|_F^2}{\|\mathbf{W}_k - \mathbf{W}_{k-1}\|_F + \|\mathbf{W}_k - \mathbf{W}_{k-1}^{L-1}\|_F} \\ & \geq \bar{C} \frac{\|\mathbf{W}_{k+1} - \mathbf{W}_k\|_F^2 + \|\mathbf{W}_{k+1} - \mathbf{W}_k^{L-1}\|_F^2}{\sqrt{\|\mathbf{W}_k - \mathbf{W}_{k-1}\|_F^2 + \|\mathbf{W}_k - \mathbf{W}_{k-1}^{L-1}\|_F^2}}, \end{aligned} \quad (25)$$

where the second inequality uses Lemma 2 and (24), the third inequality is due to Lemma 6, and \bar{C} in the last line is

$$\bar{C} = \frac{\lambda(1-\theta)}{8lrC_3(2B_0 + \lambda + \|\mathbf{X}\|_F)} > 0.$$

Due to $\frac{a}{t} = \frac{a}{t} + t - t \geq 2\sqrt{a} - t$ for all $a \geq 0, t > 0$, we have

$$\begin{aligned} & \frac{\|\mathbf{W}_{k+1} - \mathbf{W}_k\|_F^2 + \|\mathbf{W}_{k+1} - \mathbf{W}_k^{L-1}\|_F^2}{\sqrt{\|\mathbf{W}_k - \mathbf{W}_{k-1}\|_F^2 + \|\mathbf{W}_k - \mathbf{W}_{k-1}^{L-1}\|_F^2}} \\ & \geq 2\sqrt{\|\mathbf{W}_{k+1} - \mathbf{W}_k\|_F^2 + \|\mathbf{W}_{k+1} - \mathbf{W}_k^{L-1}\|_F^2} \\ & \quad - \sqrt{\|\mathbf{W}_k - \mathbf{W}_{k-1}\|_F^2 + \|\mathbf{W}_k - \mathbf{W}_{k-1}^{L-1}\|_F^2} \end{aligned} \quad (26)$$

Combining (25) and (26) and summing them up from $\tilde{k} \geq k_0$ to $m \rightarrow \infty$ yields

$$\begin{aligned} & \sum_{k=\tilde{k}}^{\infty} \sqrt{\|\mathbf{W}_{k+1} - \mathbf{W}_k\|_F^2 + \|\mathbf{W}_{k+1} - \mathbf{W}_k^{L-1}\|_F^2} \\ & \leq \sqrt{\|\mathbf{W}_{\tilde{k}} - \mathbf{W}_{\tilde{k}-1}\|_F^2 + \|\mathbf{W}_{\tilde{k}} - \mathbf{W}_{\tilde{k}-1}^{L-1}\|_F^2} \\ & \quad + \frac{1}{\bar{C}} (f(\mathbf{W}_{\tilde{k}}) - f(\mathbf{W}^*))^{1-\theta}, \end{aligned} \quad (27)$$

which immediately implies

$$\sum_{k=\tilde{k}}^{\infty} \|\mathbf{W}_{k+1} - \mathbf{W}_k\|_F < \infty.$$

Thus, we conclude that $\{\mathbf{W}_k\}_{k \geq 0}$ is a Cauchy sequence and hence is convergent. It immediately follows that the limit points set $\mathcal{C}(\mathbf{W}_0) = \{\mathbf{W}^*\}$ is a singleton and $\mathbf{W}^* = (\mathbf{U}^*, \mathbf{V}^*)$ is a critical point of (3) due to Lemma 8.

As for convergence rate, it follows from (27) that

$$\begin{aligned} & \|\mathbf{W}_{\tilde{k}} - \mathbf{W}^*\|_F \\ & \leq \sum_{k=\tilde{k}}^{\infty} \sqrt{\|\mathbf{W}_{k+1} - \mathbf{W}_k\|_F^2 + \|\mathbf{W}_{k+1} - \mathbf{W}_k^{L-1}\|_F^2} \\ & \leq \sqrt{\|\mathbf{W}_{\tilde{k}} - \mathbf{W}_{\tilde{k}-1}\|_F^2 + \|\mathbf{W}_{\tilde{k}} - \mathbf{W}_{\tilde{k}-1}^{L-1}\|_F^2} \\ & \quad + \alpha \left(\sqrt{\|\mathbf{W}_{\tilde{k}} - \mathbf{W}_{\tilde{k}-1}\|_F^2 + \|\mathbf{W}_{\tilde{k}} - \mathbf{W}_{\tilde{k}-1}^{L-1}\|_F^2} \right)^{\frac{1-\theta}{\theta}} \end{aligned} \quad (28)$$

for some constant $\alpha > 0$, where the last line uses (24) and Lemma 6. Denoting by

$$P_{\tilde{k}} = \sum_{k=\tilde{k}}^{\infty} \sqrt{\|\mathbf{W}_{k+1} - \mathbf{W}_k\|_F^2 + \|\mathbf{W}_{k+1} - \mathbf{W}_k^{L-1}\|_F^2},$$

we obtain

$$P_k \leq P_{k-1} - P_k + \alpha \left[P_{k-1} - P_k \right]^{\frac{1-\theta}{\theta}}. \quad (29)$$

The above recursion about the sequence $\{P_k\}_{k \geq k_0}$ has exactly the same form with [32, eq. (12)]. Hence the convergence rate can be obtained by following the same arguments after [32, eq. (12)]. This completes the proof. \square

6 CONCLUSION

In order to design efficient alternating-type algorithms for the symmetric NMF, we transfer this problem to a penalized nonsymmetric NMF. We have proved that solving the nonsymmetric reformulation returns a solution for the original symmetric NMF when the penalty term is relatively large, in sharp contrast to the classical result for the methods of Lagrangian multiplier that suggests it happens only when the penalty term tends to infinity. Furthermore, we have proved that various alternating-type algorithms—when used to efficiently solve the nonsymmetric reformulation—admit strong convergence guarantee in the sense that the generated sequence is convergent at least at a sublinear rate and it converges to a critical point of the original symmetric NMF. An interesting question would be whether it is possible to further improve the lower bound on the penalty parameter λ that ensures convergence, and even to the extreme case that whether the convergence to a critical point of the original symmetric NMF is guaranteed for any positive λ . In additions, it would also be of great interest to extend both algorithmic strategy and theoretical guarantee for multidimensional cases, such as symmetric tensor factorization and symmetric nonnegative tensor factorization.

ACKNOWLEDGMENT

We gratefully acknowledge Dr. Songtao Lu for sharing the code used in [28], and the four anonymous reviewers for their constructive comments. X. Li is partially supported by the National Natural Science Foundation of China (NSFC) grant NSFC-72150002 and by AC01202101037 and AC01202108001 from Shenzhen Institute of Artificial Intelligence and Robotics for Society (AIRS). Z. Zhu is partially supported by the NSF grants CCF2106881 and CCF 2008460.

REFERENCES

- [1] Z. Zhu, X. Li, K. Liu, and Q. Li, "Dropping symmetry for fast symmetric nonnegative matrix factorization," in *Advances in Neural Information Processing Systems*, pp. 5154–5164, 2018.
- [2] D. D. Lee and H. S. Seung, "Learning the parts of objects by non-negative matrix factorization," *Nature*, vol. 401, no. 6755, p. 788, 1999.
- [3] D. Guillamet and J. Vitria, "Non-negative matrix factorization for face recognition," in *Topics in artificial intelligence*, pp. 336–344, Springer, 2002.
- [4] F. Shahnaz, M. W. Berry, V. P. Pauca, and R. J. Plemmons, "Document clustering using nonnegative matrix factorization," *Information Processing & Management*, vol. 42, no. 2, pp. 373–386, 2006.
- [5] D. Cai, X. He, J. Han, and T. S. Huang, "Graph regularized nonnegative matrix factorization for data representation," *IEEE transactions on pattern analysis and machine intelligence*, vol. 33, no. 8, pp. 1548–1560, 2010.
- [6] H. Liu, Z. Wu, X. Li, D. Cai, and T. S. Huang, "Constrained nonnegative matrix factorization for image representation," *IEEE Transactions on Pattern Analysis and Machine Intelligence*, vol. 34, no. 7, pp. 1299–1311, 2011.
- [7] X. Li, M. Chen, and Q. Wang, "Discrimination-aware projected matrix factorization," *IEEE Transactions on Knowledge and Data Engineering*, vol. 32, no. 4, pp. 809–814, 2019.
- [8] Q. Wang, X. He, X. Jiang, and X. Li, "Robust bi-stochastic graph regularized matrix factorization for data clustering," *IEEE Transactions on Pattern Analysis and Machine Intelligence*, 2020.
- [9] C. Févotte, N. Bertin, and J.-L. Durrieu, "Nonnegative matrix factorization with the itakura-saito divergence: With application to music analysis," *Neural computation*, vol. 21, no. 3, pp. 793–830, 2009.
- [10] W.-K. Ma, J. M. Bioucas-Dias, T.-H. Chan, N. Gillis, P. Gader, A. J. Plaza, A. Ambikapathi, and C.-Y. Chi, "A signal processing perspective on hyperspectral unmixing: Insights from remote sensing," *IEEE Signal Processing Magazine*, vol. 31, no. 1, pp. 67–81, 2014.
- [11] N. Gillis, "The why and how of nonnegative matrix factorization," *Regularization, Optimization, Kernels, and Support Vector Machines*, vol. 12, no. 257, 2014.
- [12] D. D. Lee and H. S. Seung, "Algorithms for non-negative matrix factorization," in *Advances in neural information processing systems*, pp. 556–562, 2001.
- [13] C.-J. Lin, "Projected gradient methods for nonnegative matrix factorization," *Neural computation*, vol. 19, no. 10, pp. 2756–2779, 2007.
- [14] J. Kim and H. Park, "Toward faster nonnegative matrix factorization: A new algorithm and comparisons," in *International Conference on Data Mining*, pp. 353–362, 2008.
- [15] A. Cichocki and A.-H. Phan, "Fast local algorithms for large scale nonnegative matrix and tensor factorizations," *IEICE transactions on fundamentals of electronics, communications and computer sciences*, vol. 92, no. 3, pp. 708–721, 2009.
- [16] C. Ding, X. He, and H. D. Simon, "On the equivalence of nonnegative matrix factorization and spectral clustering," in *Proceedings of International Conference on Data Mining*, pp. 606–610, 2005.
- [17] Z. He, S. Xie, R. Zdunek, G. Zhou, and A. Cichocki, "Symmetric nonnegative matrix factorization: Algorithms and applications to probabilistic clustering," *IEEE Transactions on Neural Networks*, vol. 22, no. 12, pp. 2117–2131, 2011.
- [18] D. Kuang, S. Yun, and H. Park, "Symnmf: nonnegative low-rank approximation of a similarity matrix for graph clustering," *Journal of Global Optimization*, vol. 62, no. 3, pp. 545–574, 2015.
- [19] X. Luo, M. Shang, et al., "Symmetric non-negative latent factor models for undirected large networks," in *IJCAI*, pp. 2435–2442, 2017.
- [20] L. Hu and G. Guo, "An augmented lagrangian alternating direction method for overlapping community detection based on symmetric nonnegative matrix factorization," *International Journal of Machine Learning and Cybernetics*, vol. 11, no. 2, pp. 403–415, 2020.
- [21] J. Nocedal and S. Wright, *Numerical optimization*. Springer Science & Business Media, 2006.
- [22] N. Gillis and F. Glineur, "Accelerated multiplicative updates and hierarchical als algorithms for nonnegative matrix factorization," *Neural computation*, vol. 24, no. 4, pp. 1085–1105, 2012.
- [23] H. Attouch, J. Bolte, P. Redont, and A. Soubeyran, "Proximal alternating minimization and projection methods for nonconvex problems: An approach based on the kurdyka-łojasiewicz inequality," *Mathematics of Operations Research*, vol. 35, no. 2, pp. 438–457, 2010.
- [24] J. Bolte, S. Sabach, and M. Teboulle, "Proximal alternating linearized minimization for nonconvex and nonsmooth problems," *Mathematical Programming*, vol. 146, no. 1-2, pp. 459–494, 2014.
- [25] A. Vandaele, N. Gillis, Q. Lei, K. Zhong, and I. Dhillon, "Efficient and non-convex coordinate descent for symmetric nonnegative matrix factorization," *IEEE Transactions on Signal Processing*, vol. 64, no. 21, pp. 5571–5584, 2016.
- [26] K. Huang, N. D. Sidiropoulos, and A. Swami, "Non-negative matrix factorization revisited: Uniqueness and algorithm for symmetric decomposition," *IEEE Transactions on Signal Processing*, vol. 62, no. 1, pp. 211–224, 2013.
- [27] R. Borhani, J. Watt, and A. Katsaggelos, "Fast and effective algorithms for symmetric nonnegative matrix factorization," *arXiv preprint arXiv:1609.05342*, 2016.

- [28] S. Lu, M. Hong, and Z. Wang, "A nonconvex splitting method for symmetric nonnegative matrix factorization: Convergence analysis and optimality," *IEEE Transactions on Signal Processing*, vol. 65, no. 12, pp. 3120–3135, 2017.
- [29] K. Huang, N. D. Sidiropoulos, and A. P. Liavas, "A flexible and efficient algorithmic framework for constrained matrix and tensor factorization," *IEEE Transactions on Signal Processing*, vol. 64, no. 19, pp. 5052–5065, 2016.
- [30] M. Razaviyayn, M. Hong, and Z.-Q. Luo, "A unified convergence analysis of block successive minimization methods for nonsmooth optimization," *SIAM J. Optimization*, vol. 23, no. 2, pp. 1126–1153, 2013.
- [31] S.-D. Wang, T.-S. Kuo, and C.-F. Hsu, "Trace bounds on the solution of the algebraic matrix riccati and lyapunov equation," *IEEE Transactions on Automatic Control*, vol. 31, no. 7, pp. 654–656, 1986.
- [32] H. Attouch and J. Bolte, "On the convergence of the proximal algorithm for nonsmooth functions involving analytic features," *Mathematical Programming*, vol. 116, no. 1, pp. 5–16, 2009.
- [33] W. Xu, X. Liu, and Y. Gong, "Document clustering based on non-negative matrix factorization," in *International ACM SIGIR conference on Research and development in information retrieval*, pp. 267–273, 2003.
- [34] J. Bolte, A. Daniilidis, and A. Lewis, "The Łojasiewicz inequality for nonsmooth subanalytic functions with applications to subgradient dynamical systems," *SIAM Journal on Optimization*, vol. 17, no. 4, pp. 1205–1223, 2007.
- [35] H. Attouch, J. Bolte, and B. F. Svaiter, "Convergence of descent methods for semi-algebraic and tame problems: proximal algorithms, forward-backward splitting, and regularized gauss–seidel methods," *Mathematical Programming*, vol. 137, no. 1-2, pp. 91–129, 2013.